ISSN 1349-1237

SCIENCE REPORTS OF NIIGATA UNIVERSITY

(GEOLOGY)

No. 39 (2024)

Published
by
The Department of Geology, Faculty of Science
Niigata University, Niigata, Japan

31 March 2024

All communications relating to this report should be addressed to:
The editor of
"Science Reports of Niigata University (Geology)"
Department of Geology, Faculty of Science, Niigata University
Niigata 950-2181, Japan

An elementary approach for estimating fossil volume: implications for allometric scaling

Kota SATO*, Rintaro FUKUTA** and Yuta SHIINO*

Abstract

To calculate the volume of fossils based on Archimedes' principle, a simple experimental system for measuring underwater weight was constructed using a pole stand and a digital balance. As an initial step to examine fossil specimens, we validated the experimental system using 1 cm^3 metal cubes made of aluminium and iron. The average underwater weights of the aluminium and iron cubes were 0.997 g and 1.006 g, respectively. Utilising the density of fresh water, we determined the volumes calculated from underwater weights to be 1.001 cm^3 for the aluminium cube and 0.992 cm^3 for the iron cube, both of which corresponded to the product information for the metal cubes. Subsequently, when applying the experimental system to fossil specimens of the strophomenid brachiopod *Eoplectodonta transversalis*, our results indicated that the length and width of the shell exhibited an isometric and negative growth relationship relative to its volume, respectively. This morphological trend could potentially be attributed to the development of the ptycholophous lophophore, which caused a commensurate anterior growth to accommodate the increased metabolic rate.

Key words: Allometry, Brachiopoda, Strophomenida, Silurian, morphology, growth strategy.

* Department of Geology, Faculty of Science, Niigata University, Niigata 950-2181, Japan
** Graduate School of Science and Technology, Niigata University, Niigata 950-2181, Japan

Corresponding author: Y. Shiino,
y-shiino@geo.sc.niigata-u.ac.jp

(Manuscript received 3 October, 2023; accepted 20 January, 2024)

Introduction

Biomechanical approaches to fossil organisms significantly contribute to our understanding of adaptation and evolution in palaeontology (e.g., Koehl, 1996; Shiino et al., 2009, 2014; Fujiwara and Hutchinson, 2012). Because this approach allows numerical determination of functional thresholds and applicable ranges for adaptation capability and biological performance, the concept of treating an organism as a functionally integrated body serves as the "workhorse" of the functional morphological analyses (e.g., Shiino and Kuwazuru, 2010, 2011; Shiino et al., 2012). However, all organisms change their size and form during growth, which contrasts with mechanical designs that remain morphologically unchanged from production to disposal. The variable systems involved in the morphology of organisms do not collapse into dysfunction and continue to be maintained while changing size; additionally, and all systems maintain a balance without contradiction or fatal conflict. Biological scaling needs to be considered to understand biological design and its related ecology and evolution within the body plan.

Brachiopods are good examples for the study of biological scaling because their shells preserve their growth history as accrementition, showing a variety of morphology in terms of outline and convexity (Williams et al., 1997b). In general, the length of brachiopod shells is assumed to represent the size parameter for scaling (e.g., Zezina and Smirnova, 1977; Peck and Holmes, 1989; Saito and Tazawa, 2002). On the other hand, most of the interior of rhynchonelliformean brachiopods is a mantle cavity, which contains a tentaculate feeding organ, so called the lophophore (James et al., 1992; Williams et al., 1997b). Consequently, the total volume encapsulated by the shell is significantly correlated with the space available for filter feeding, which may be indicative of metabolic rates during growth.

For calculating the volume of an object, the underwater weight warrants consideration based on Archimedes' principle. When an object is submerged in water, the surrounding water exerts an upward buoyant force on the object (e.g., Ichinohe et al., 2019). Simultaneously, a downward force equal to the buoyant force acts on the water as a reaction. According to Archimedes' principle, the buoyant force is equal to the weight of the volume of the liquid displaced by the object. Therefore, the volume of an object based on its underwater weight can be calculated and represents the weight of the liquid displaced by the object.

As a preliminary step to understand growth strategies in fossil brachiopods, we constructed a simple experimental system to calculate the underwater weight of objects. Based on the validity and repeatability of the present system, we examined the growth pattern of Silurian brachiopods, with special reference to allometric scaling.

Material and methods

1. Metal material and fossil specimens

For the test experiments, we used aluminium and iron cubes of 1 cm^3, Density Measurement Cube (Artec Co., Ltd., Japan). The tolerances of these cubes are ±5%. We used 2.699 g/cm^3 and 7.874 g/cm^3 for the densities of aluminium and iron cubes, respectively.

For the examination of allometric scaling, we used 43 specimens of fossil brachiopod *Eoplectodonta transversalis* (Wahlenberg, 1818) from the lower Silurian Visby Formation of Gotland, Sweden (Fig. 1). All specimens have well-preserved conjoined valves, with size ranging from 2.12–12.28 mm in length. Prior to the calculation, nearly all the muddy particles on the specimens were removed using an ultrasonic cleaner.

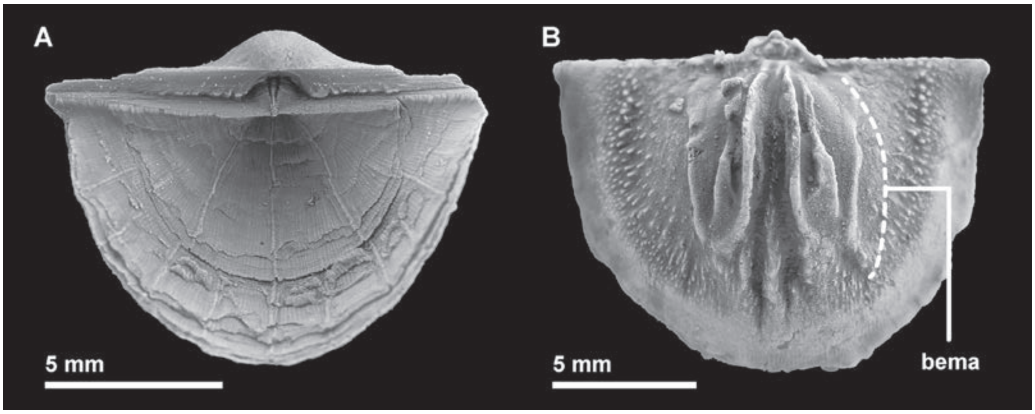

Fig. 1. Morphology of fossil brachiopod *Eoplectodonta transversalis* (Wahlenberg, 1818). **A**. Dorsal view of conjoined shell. **B**. Ventral (internal) view of dorsal valve. Several rows of the ridges, called bema, are attachment sites of ptycholophous lophophore. Photographs referenced from Shiino (2013).

2. Experimental protocols

To calculate the underwater weight of the fossil specimens, a simple experimental system using a pole stand and a digital balance was constructed (Fig. 2). The pole stand was equipped with a small stage with an iron beam (Fig. 2B). The stage was slightly submerged in a beaker filled with water in advance, and its weight was measured using a digital scale Precision Balance RJ-320 (Shinko Denshi Co., Ltd., Japan). Subsequently, the specimen was placed on the stage and slowly submerged, and the underwater weight was measured.

To examine the effect of rocks absorbing water, the differences in the underwater weights of the dry and wet specimens were compared. The weight of the fossil itself was also measured and compared with the volume calculated using the density of fossil. The shells of rhynchonelliformean brachiopods are primarily composed of calcium carbonate in the form of low-magnesian calcite (Jope, 1965). Furthermore, the present specimens occur in marlstone without sedimentary structures. Although there may be heterogeneity of

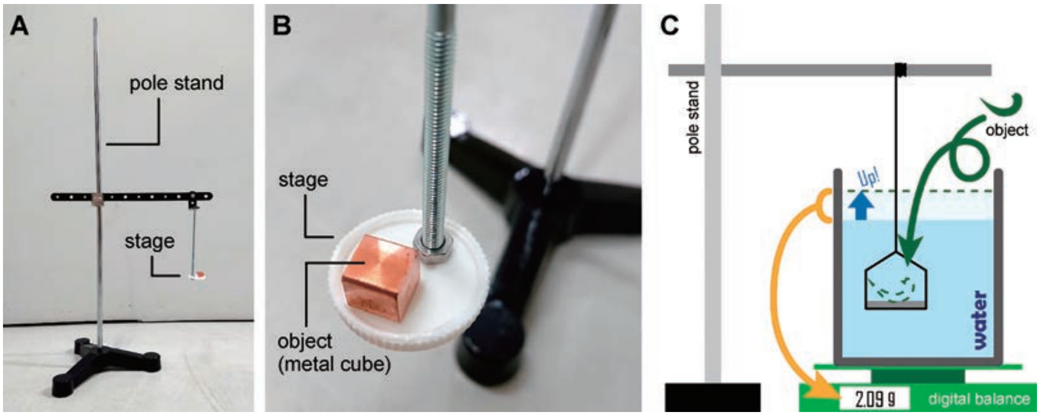

Fig. 2. Experimental system to calculate the underwater weight. **A**. Photograph of the experimental system without an electronic balance. **B**. Magnified photograph of the stage. **C**. Schematic illustration of the experimental system.

material inside the shell, we utilised the ideal density of calcite (2.71 g/cm^3) to estimate the volume based on the weight of the fossil.

3. Evaluation of brachiopod morphology

To evaluate the growth of *Eoplectodonta transversalis*, we measured the length L and width W using photographs of each specimen, and these measurements were compared with the calculated volume using the underwater weight. In the case of biological scaling, two variables of morphometric data were typically plotted on logarithmic coordinates, resulting in the linear-regression lines of the allometric equation, $y = ax^b$, where x and y are variables (Schmidt-Nielsen, 1984). Therefore, the graphs are shown with a double-logarithmic scale.

In general, component b in the allometric equation reflects the difference in growth strategy. When we compared two variables of the same dimension, such as a length relative to another length, a component greater than 1 could be interpreted as positive allometric growth, a component close to 1 could be interpreted as isometric growth, and a component smaller than 1 could be interpreted as negative allometric growth. The threshold value of the isometric growth differs in their dimensions; the volume increases as the cube of the length.

4. Statistical analysis

Statistical analyses were performed using R (The R Foundation for Statistical Computing, Vienna, Austria, version 4.2.1). To find correlations among the parameters, we conducted Pearson's correlation tests and set the significance level p-value at 0.05.

Results and discussion

1. Metal cubes

Table 1 shows the underwater weights of six experiments using aluminium and iron cubes. The range of numerical values for the aluminium cube was 0.978–1.054 g, with an average of 0.997 g, and the range of numerical values for the iron cube was 0.987–1.041 g, with an average of 1.006 g. Figure 3 shows box plots of the underwater weight using the aluminium and iron cubes. In both cubes, no significant differences were observed between the six experiments.

Table 2 shows numerical values of the volume V based on density D and weight M and the calculated volume Vu based on the average underwater weight Mu. The calculated volume Vu of the aluminium cube was 1.001 cm^3 and that of the iron cube was 0.992 cm^3, both of which were similar to those of volume V. Therefore, our method could be applied to ensure the experimental validity of using the underwater weight to calculate its volume.

Table 1. Numerical values of underwater weight using aluminium and iron cubes.

Material	1 [g]	2 [g]	3 [g]	4 [g]	5 [g]	6 [g]	Average underwater weight Mu [g]
Al	0.984	0.985	0.985	1.054	0.994	0.978	0.997
Fe	1.041	0.989	1.001	0.987	1.033	0.987	1.006

We demonstrated six times measurements, and then calculated average values.

Table 2. Numerical values of the test experiments using aluminium and iron cubes.

Material	Density D [g/cm^3]	Weight M [g]	Volume V (=D/M) [cm^3]	Average underwater weight Mu [g]	Calculated volume Vu (=Mu/0.998) [cm^3]	Difference rate (Vu-V)/V
Al	2.699	2.677	0.992	0.997	1.001	0.009
Fe	7.874	7.699	0.978	1.006	0.992	0.014

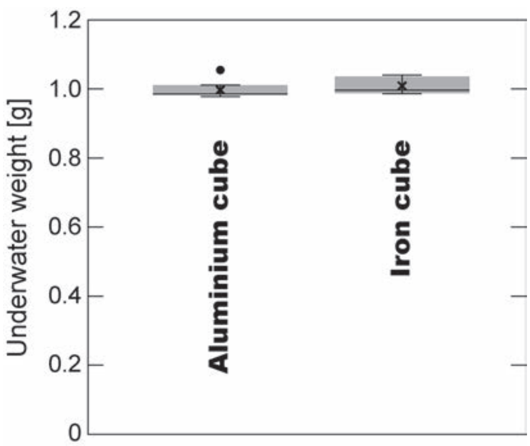

Fig. 3. Box plots of the numerical values using aluminium and iron cubes. The vertical lines with terminal cross bars are maximum and minimum values with the exception of an outlier value (black coloured circle). The lower and upper ends of each box indicate the 1st and 3rd quartiles, respectively. In each box, the horizontal black line shows the median, while the cross mark shows the average.

Table 3. Morphometric values of brachiopod *Eoplectodonta transversalis*.

Specimen ID	Length L [mm]	Width W [mm]	Weight M_f [g]	Volume V_s (= M_f/2.71) [cm³]	Underwater weight of dry specimen M_{ds} [g]	Underwater weight of wet specimen M_{ws} [g]	Calculated volume of dry specimen V_{df} (= M_{ds}/0.998) [cm³]	Calculated volume of wet specimen V_{ws} (= M_{ws}/0.998) [cm³]
1	2.12	3.18	0.003	0.00111	---	0.001	---	0.00100
2	4.20	8.20	0.025	0.00923	0.005	0.008	0.00501	0.00802
3	3.92	6.13	0.018	0.00664	0.005	0.005	0.00501	0.00501
4	6.22	9.68	0.077	0.02841	0.026	0.028	0.02605	0.02806
5	5.60	9.83	0.055	0.02030	0.026	0.021	0.02605	0.02104
6	6.48	9.58	0.080	0.02952	0.032	0.030	0.03206	0.03006
7	3.78	7.14	0.016	0.00590	0.007	0.009	0.00701	0.00902
8	4.40	7.16	0.022	0.00812	0.008	0.009	0.00802	0.00902
9	3.12	5.15	0.005	0.00185	0.006	0.004	0.00601	0.00401
10	5.00	7.83	0.046	0.01697	0.016	0.018	0.01603	0.01804
11	11.11	12.99	0.378	0.13948	0.150	0.151	0.15030	0.15130
12	7.80	11.63	0.151	0.05572	0.056	0.057	0.05611	0.05711
13	8.42	10.91	0.208	0.07675	0.079	0.081	0.07916	0.08116
14	7.04	9.70	0.090	0.03321	0.026	0.036	0.02605	0.03607
15	4.86	7.55	0.038	0.01402	0.013	0.014	0.01303	0.01403
16	8.61	12.57	0.174	0.06421	0.065	0.066	0.06513	0.06613
17	11.25	13.05	0.424	0.15646	0.163	0.163	0.16333	0.16333
18	5.48	9.02	0.049	0.01808	0.021	0.016	0.02104	0.01603
19	7.03	10.85	0.105	0.03875	0.040	0.042	0.04008	0.04208
20	9.81	11.01	0.314	0.11587	0.119	0.120	0.11924	0.12024
21	5.28	8.66	0.037	0.01365	0.011	0.016	0.01102	0.01603
22	11.06	12.88	0.388	0.14317	0.140	0.149	0.14014	0.14915
23	8.91	12.14	0.180	0.06642	0.076	0.078	0.07608	0.07808
24	5.35	8.30	0.046	0.01697	0.008	0.020	0.00801	0.02002
25	6.73	10.15	0.096	0.03542	0.037	0.041	0.03704	0.04104
26	11.12	13.89	0.454	0.16753	0.179	0.181	0.17918	0.18118
27	6.77	9.33	0.077	0.02841	0.036	0.034	0.03604	0.03403
28	11.16	12.34	0.444	0.16384	0.180	0.183	0.18018	0.18318
29	11.35	12.20	0.369	0.13616	0.145	0.139	0.14515	0.13914
30	10.24	11.94	0.434	0.16015	0.158	0.165	0.15816	0.16517
31	10.25	11.19	0.313	0.11550	0.128	0.125	0.12813	0.12513

Specimen ID	Length L [mm]	Width W [mm]	Weight M_f [g]	Volume V_s (=M_f/2.71) [cm^3]	Underwater weight of dry specimen M_{ds} [g]	Underwater weight of wet specimen M_{ws} [g]	Calculated volume of dry specimen V_{df} (=M_{ds}/0.998) [cm^3]	Calculated volume of wet specimen V_{ws} (=M_{ws}/0.998) [cm^3]
32	9.66	11.08	0.247	0.09114	0.101	0.102	0.10110	0.10210
33	7.80	11.11	0.160	0.05904	0.069	0.065	0.06907	0.06507
34	9.50	10.57	0.267	0.09852	0.104	0.105	0.10410	0.10511
35	5.72	9.16	0.058	0.02140	0.026	0.023	0.02603	0.02302
36	12.22	13.45	0.564	0.20812	0.214	0.222	0.21421	0.22222
37	6.26	8.81	0.080	0.02952	0.027	0.034	0.02705	0.03407
38	9.48	10.06	0.253	0.09336	0.094	0.101	0.09419	0.10120
39	9.28	11.21	0.237	0.08745	0.090	0.091	0.09018	0.09118
40	9.24	14.68	0.220	0.08118	0.092	0.083	0.09218	0.08317
41	12.28	12.75	0.570	0.21033	0.216	0.218	0.21643	0.21844
42	12.25	13.82	0.497	0.18339	0.210	0.209	0.21042	0.20942
43	11.84	13.13	0.490	0.18081	0.180	0.185	0.18036	0.18537

---: unmeasurable

2. Length, width and volume of *Eoplectodonta transversalis*

The length L, width W, weight M_f, underwater weight in dry M_{ds} and wet M_{ws} conditions of all specimens were measured, with the exception of the underwater weight of the dry specimen M_{ds} for specimen ID1. Because the specimen is too small with a length of 2.12 mm, the measurement display remained zero when the specimen in the dried condition was placed on the stage in the underwater setup. Using the specimen under the wet condition, 0.001 g of underwater weight was measured, though the numerical value was a detection limit. In our present experimental system, the underwater weight of the small specimens less than 4.4 mm in length was determined to be only one significant digit.

The width W and weight M_f increased with length increased as shown in Fig. 4A, B. For the allometric equation, we obtained $W = 2.70L^{0.66}$ ($R = 0.92$, $p < 0.01$) and $M_f = (3.0 \times 10^{-4}) L^{3.05}$ ($R = 0.95$, $p < 0.01$). In the former case, the length L has a positive allometric growth with respect to the width W because the exponent value was 0.66 (Fig. 4A). Qualitatively, this indicates that the greater the length, the greater will be the elongated appearance.

Figure 4C shows the numerical values of the volume relative to the length L or width W; the volume V_s (= Mf / 2.71), the calculated volume of dry specimen V_{df} (= M_{ds} / 0.998) and the calculated volume of wet specimen V_{ws} (= M_{ws} / 0.998). We obtained $V_s = (1.0 \times 10^{-4}) L^{3.05}$ ($R = 0.95$), $V_{ds} = (1.0 \times 10^{-4}) L^{3.07}$ ($R = 0.96$), $V_{ws} = (1.0 \times 10^{-4}) L^{3.01}$ ($R = 0.95$), and $V_{ws} = (4.0 \times 10^{-6}) W^{4.04}$ ($R = 0.81$), all of which have significant correlations ($p < 0.01$).

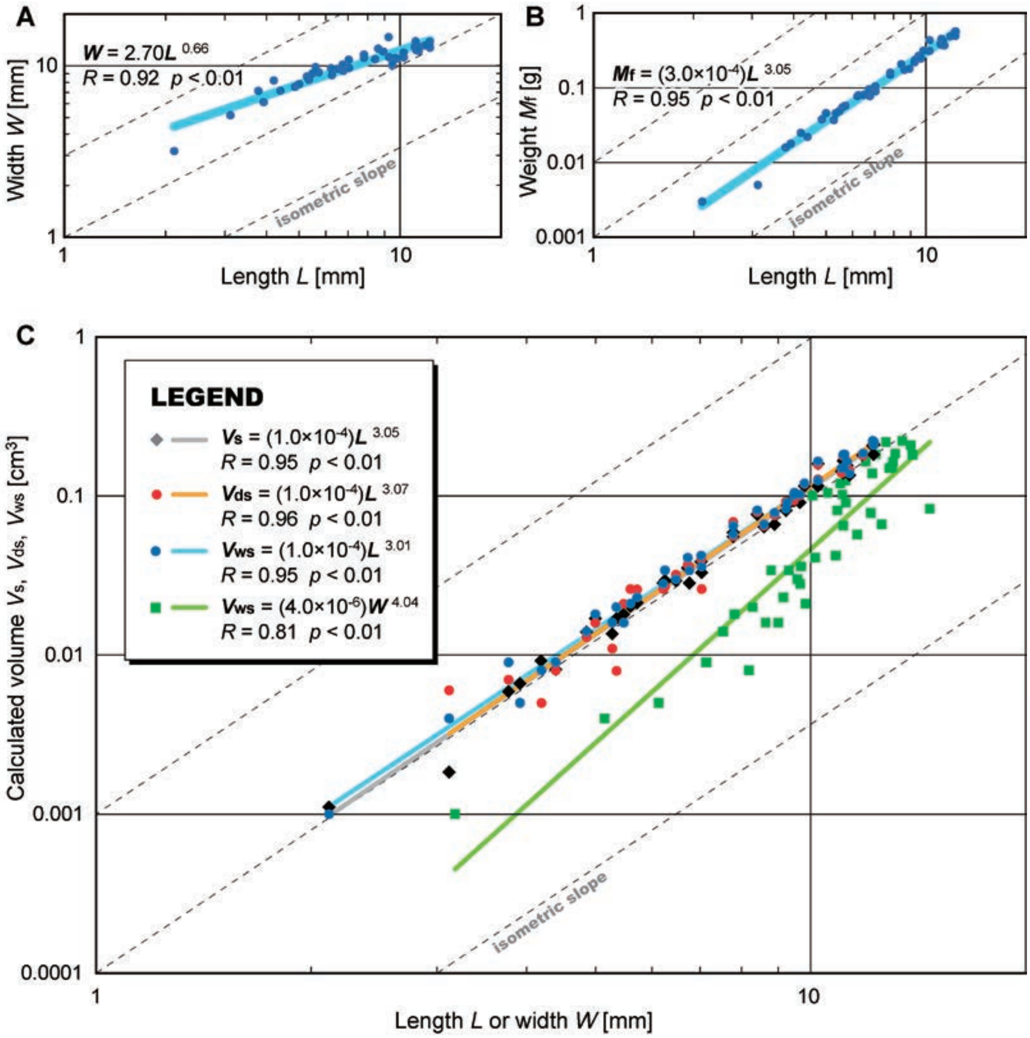

Fig. 4. Graphs of the numerical values. **A**. Width W with respect to length L ($p = 2.2 \times 10^{-16}$). **B**. Weight M_f with respect to length L ($p = 2.2 \times 10^{-16}$). **C**. Calculated volume V_s, V_{ds} and V_{ws} with respect to length L or width W. The block lines indicate the approximation with significant correlation based on the p-value.

All cases of the volume relative to length were closely similar to each other, with those components ranging from 3.01 to 3.07 (Fig. 4C). This relationship between the length and volume implies isometric growth. Unlike the comparison with length, the volume relative to width shows a larger increment in contrast to the isometric growth. Consequently, the width of the present species clearly shows a negative allometric growth with respect to either length or volume.

Several brachiopod species tend to have elongated shell outlines (e.g., Tazawa, 1974; Michalik, 1996). Because the brachiopod shell encapsulates soft parts responsible for biological performance, the changes of shell outline can be explained by the structure and function of the internal organs. The internal space of the shell is mainly subdivided into two parts; a body cavity and a mantle cavity (Williams et al., 1997b). The body cavity is a main part of the coelomic space in the posteromedian zone and contains the important organs such as muscles, digestive tract and reproductive structures (Williams et al., 1997b). The mantle cavity at the antero-lateral space inside the shell contains a food-collecting organ, called the lophophore; here, the flow of seawater enables passing (Williams et al., 1997b). In the case of typical rhynchonelliformeans including the present species, the space of the mantle cavity is greater than that of the body cavity (Williams et al., 1997b). This leads to the possibility that the difference in shell volume calculated herein is closely related to the development of the lophophore, reflecting metabolic requirements in each brachiopod species.

Eoplectodonta has a ptycholophous type of lophophore on the inner surface of the dorsal valve (Williams et al., 1997a; Clarkson, 1998). As the growth progresses, each lobe of ptycholophe extends in the anterior direction (Williams et al., 1997a). Therefore, the positive allometric growth of length relative to width can be interpreted as the development of the mantle cavity for the growth of the ptycholophous lophophore. This growth pattern could have allowed for isometric growth in length and volume, which is a similar trend to the case of extant terebratulid brachiopods (Peck and Holmes, 1989). By contrast, brachiopods with laterally extended lophophore may exhibit negative allometric growth of length relative to width. It is likely in spiriferid brachiopods with a long-winged appearance which have spiral lophophore with small diameter but larger number of spires, as observed in *Mucrospirifer* (Ager and Riggs, 1964; Carter et al., 2006).

3. Insights into the allometric scaling of brachiopod morphology

Based on Archimedes' principle, our study established a method to calculate volume based on the underwater weight. It is possible to uniformly compare three-dimensional body size data in terms of volume, even when the shapes of the objects are different. A problem is still present in the calculation of the small specimens of *Eoplectodonta* less than 4.4 mm in length; however, the volume calculated from the density of calcite and the weight of the specimen itself was effectively matched with the volume based on the underwater weight. This result indicates that the present specimens have similar physical properties to a calcareous shell and sediments with a lower amount of inside void space. By cross-checking the volume of the specimens based on the underwater weight and fossil weight, the validity of the calculated values to reflect the growth pattern of brachiopod morphology could be determined.

There are many smaller species of brachiopods. To unravel their growth strategies from morphological analysis, more advanced analysis, such as a microfocus X-ray CT, needs to be used (e.g., Shiino et al., 2020).

Acknowledgements

We gratefully acknowledge Hiroshi Kurita (Niigata University) for his helpful support of experimental facilities and thorough discussion. We also thank a reviewer Takashi Yoshino (Toyo University) and an editor Atsushi Matsuoka (Niigata University) for their constructive comments. This study was financially supported in part by the JSPS KAKENHI Grant Numbers 21K03736 and 22K03795. This study was a research activity of the "Frontier Study Project" in the Faculty of Science, Niigata University.

References

Ager, D. V. and Riggs, E. A., 1964, The internal anatomy, shell growth and asymmetry of a Devonian spiriferid. *J. Paleontol.*, **38**, 749–760.

Carter, J. L., Johnson, J. G., Gourvennec, R. and Hong-Fei, H., 2006, Spiriferida. *In* Kaesler, R. L., ed., *Treatise on Invertebrate Paleontology, Part H: Brachiopoda Revised Volume 5*, Geological Society of America and University of Kansas, Boulder and Lawrence, 1689–1870.

Clarkson, E. N. K., 1998, *Invertebrate Palaeontology and Evolution. Fourth Edition.* Blackwell Science Ltd., Bristol, 452p.

Fujiwara, S. and Hutchinson, J. R., 2012, Elbow joint adductor moment arm as an indicator of forelimb posture in extinct quadrupedal tetrapods. *Proc. R. Soc. Ser. B, Biol. Sci.*, **279**, 2561–2570.

Ichinohe, R., Shiino, Y. and Kurihara, T., 2019, Active floating with buoyancy of pseudopodia versus passive floating by hydrodynamic drag force: A case study of the flat-shaped spumellarian radiolarian *Dictyocoryne*. *Paleontol. Res.*, **23**, 236–244.

James, M. A., Ansell, A. D., Curry, G. B., Collins, M. J., Peck, L. S. and Rhodes, M. C., 1992, The biology of living brachiopods. *Adv. Mar. Biol.*, **28**, 175–387.

Jope, H. M., 1965, Composition of brachiopod shell. *In* Moore, R. C., ed., *Treatise on Invertebrate Paleontology. Part H, Brachiopoda*, Geological Society of America and University of Kansas, Boulder and Lawrence, 156–164.

Koehl, M. A. R., 1996, When does morphology matter? *Ann. Rev. Ecol. Syst.*, **27**, 501–542.

Michalik, J., 1996, Functional morphology–paleoecology of pygopid brachiopods from the western Carpathian Mesozoic. *In* Copper, P. and Jin, J., eds., *Brachiopods*, A. A. Balkema, Rotterdam, 175–178.

Peck, L. S. and Holmes, L. J., 1989, Scaling patterns in the Antarctic brachiopod *Liothyrella uva* (Broderip, 1833). *J. Exp. Mar. Biol. Ecol.*, **133**, 141–150.

Saito, M. and Tazawa, J., 2002, *Hemithiris woodwardi* (A. Adams) (Rhynchonellida, Brachiopoda) from the Pleistocene Shichiba Formation, Sado Island, central Japan. *Sci. Rep., Niigata Univ. (Geol.)*, no. 17, 7–15.

Schmidt-Nielsen, K., 1984, *Scaling: Why is Animal Size so Important?* Cambridge University Press, Cambridge, 241p.

Shiino, Y., 2013, *The Mystery of Concavo-Convex Shell—Exploring Fossil Brachiopods.* Tokai University Press, Hadano, 268p. (in Japanese).

Shiino, Y. and Kuwazuru, O., 2010, Functional adaptation of spiriferide brachiopod morphology. *J. Evolution. Biol.*, **23**, 1547–1557.

Shiino, Y. and Kuwazuru, O., 2011, Theoretical approach to the functional optimisation of spiriferide brachiopod shell: Optimum morphology of sulcus. *J. Theor. Biol.*, **276**, 192–198.

Shiino, Y., Kurihara, T., Ichinohe, R., Kishimoto, N., Yoshino, T. and Matsuoka, A., 2020, A morphological analysis of the flat-shaped spumellarian radiolarian *Dictyocoryne*: morpho-functional insights into planktonic mode of life. *Paleontol. Res.*, **24**, 134–146.

Shiino, Y., Kuwazuru, O. and Yoshikawa, N., 2009, Computational fluid dynamics simulations on a Devonian spiriferid *Paraspirifer bownockeri* (Brachiopoda): Generating mechanism of passive feeding flows. *J.*

Theor. Biol., **259**, 132–141.

Shiino, Y., Kuwazuru, O., Suzuki, Y. and Ono, S., 2012, Swimming capability of the remopleuridid trilobite *Hypodicranotus striatus*: Hydrodynamic functions of the exoskeleton and the long, forked hypostome. *J. Theor. Biol.*, **300**, 29–38.

Shiino, Y., Kuwazuru, O., Suzuki, Y., Ono, S. and Masuda, C., 2014, Pelagic or benthic? Mode of life of the remopleuridid trilobite *Hypodicranotus striatulus*. *B. Geosci.*, **89**, 207–218.

Tazawa, J., 1974, *Waagenoconcha* (Brachiopoda) from the Permian of the Southern Kitakami Mountains, northeast Japan. *Jour. Fac. Sci. Hokkaido Univ. (Geol. Mineral.)*, **16**, 121–144.

Wahlenberg, G., 1818, Petrificata telluris Suecanae. *Nova Acta Regiae Societatis Scientiarum Upsaliensis*, **8** (for 1821), 1–116.

Williams, A., Brunton, C. H. C. and MacKinnon, D. I., 1997a, Morphology. *In* Kaesler, R. L., ed., *Treatise on Invertebrate Paleontology, Part H: Brachiopoda Revised Volume 1*, Geological Society of America and University of Kansas, Boulder and Lawrence, 321–422.

Williams, A., James, M. A., Emig, C. C., Mackay, S. and Rhodes, M. C., 1997b, Anatomy. *In* Kaesler, R. L., ed., *Treatise on Invertebrate Paleontology, Part H: Brachiopoda Revised Volume 1*, Geological Society of America and University of Kansas, Boulder and Lawrence, 7–188.

Zezina, O. N. and Smirnova, T. N., 1977, On the taxonomy and distribution of the Family Basiliolidae (Brachiopoda, Rhynchonellida). *Byulleten' Moskovskogo Obshchestva Ispytatelei Prirody. Otdel Biologicheskii*, **82**, 64–72 (in Russian with English abstract).

Molluscan shells on Ikarashi beach, Niigata, Japan

Toa NAKAMURA*, Yusaku HIROTA*, Souma KANEKO*, Izumi MAKIEDA*, Yoshino ISHIZAKI** and Yuta SHIINO*

Abstract

It has been suggested that beachcombing for biological material is a simple, powerful approach to understanding shallow marine ecosystems. Because of the lack of information on the molluscan shells that have washed up along the beach of the Sea of Japan, we presented a list of molluscan species collected from Ikarashi beach, Niigata, Japan. Using the molluscan shells collected between 2014 and 2023, a total of 123 species were identified: 40 gastropods, 3 cephalopods, 2 scaphopods and 78 bivalves at the species level. Several freshwater species are believed to have been possibly transported via the nearby Shin-kawa River. Holoplanktonic and nektobenthic species originally inhabited temperate sea, suggesting drift along the Tsushima Warm Current. Because benthic animals have changed their distribution in the Sea of Japan, episodic reports of molluscan fauna washing up on beaches could help to understand the environmental changes associated with the seawater temperature.

Key words: flotsam, Mollusca, Sea of Japan, Tsushima Current, beachcombing.

* Department of Geology, Faculty of Science, Niigata University, Niigata 950-2181, Japan

** Department of Earth and Planetary Science, Graduate School of Science, The University of Tokyo, Tokyo 113-0033, Japan

Corresponding author: Yuta Shiino,
y-shiino@geo.sc.niigata-u.ac.jp
(Manuscript received 4 January, 2024; accepted 8 February, 2024)

Introduction

Understanding biodiversity in ecosystems is crucial not only for monitoring current environmental conditions but also for predicting biological resources (e.g., Desa, 2016). Beachcombing is a powerful and simple monitoring technique in which shallow marine biota washed up on a beach (e.g., Donovan, 2011; Seo and Tanangonan, 2014; Yoshioka, 2016; Davies et al., 2022; Ishizaki and Shiino, 2023), although the material lacks information of spatial distribution under the sea. This approach requires the periodic recording of marine biota, and it enables the provision of basic knowledge about the relationship between local evidence and global environmental changes.

Molluscs are one of the major taxonomic groups of modern benthic fauna. There are many ecological studies on habitat depth and adaptation to environment, which are utilised to understand the marine environment and how it changes over time (e.g., Amano, 2001; Okutani, 2017; Enya and Suzuki, 2020). Molluscan shells washed up on beaches have been reported along the Sea of Japan (e.g., Takagi, 1992; Amano, 2001; Takada et al., 2015), while there is less information on molluscan shells collected from the area between Hokkaido and Niigata, except for living molluscs (Takada et al., 2015). The aim of this study is to create a database of molluscan shells collected from Ikarashi beach, Niigata, Japan.

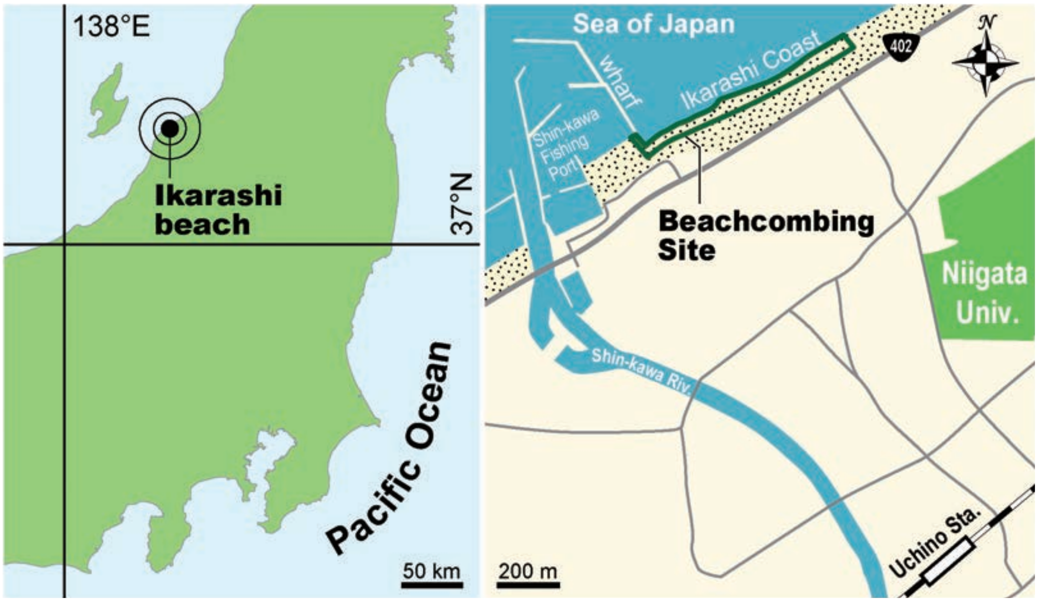

Fig. 1. Map showing the beachcombing site of Ikarashi beach, Niigata, Japan. Modified from Ishizaki and Shiino (2023).

Material and methods

1. Sampling locality

Molluscan shells were collected from 2014 to 2023 at Ikarashi beach, Niigata, Japan, located 900 m northwest of Niigata University (Fig. 1). Ikarashi beach consists mainly of fine-grained sand with abundant flotsam such as fishing tools, bottles, driftwoods and organic material (Ishizaki et al., 2023; Ishizaki and Shiino, 2023). Terrestrial organisms and products such as Chinese pond turtles and ceramics sometimes wash up on beaches after storms. Ikarashi beach's topography changes seasonally, with sand grains accumulating in summer and being removed in winter. The drift lines at which the molluscan shells wash up on the backshore vary within a backshore. The assemblage of molluscan shells differs on each drift line because the wave influences change during the tidal cycle.

2. Identification of molluscan shells

We identified the species of all the molluscan specimens stored in 200 L containers. Before identification, we cleaned the specimens with freshwater to remove sand and other unknown material unrelated to the molluscan shells. A Sony α7R IV digital camera (Sony Corporation, Japan) was used to make photographic plates of the present collection. We used a MACRO Nikkor 120 mm F6.3 lens (Nikon, Japan) for larger specimens and a MACRO Nikkor 35 mm F4.5 lens (Nikon, Japan) for specimens less than 5 mm in length; both lenses were equipped with auto bellows (Canon, Japan).

The identification of the present marine molluscs was based on Okutani (2017). The nomenclature was also based on Okutani (2017), except for some species that have recently been revised to different names. Although the molluscan shells were collected from the beach, our collection includes several species of freshwater molluscs. The nomenclature of the freshwater species was based on Okutani (2004).

All the specimens are stored in the collections of Palaeontology Laboratory by the last author, Niigata University.

Table 1. List of molluscan species.

Class	Oder	Family	Species	Japanese name	Plate and figure number
Gastropoda	Patellogastropoda	Nacellidae	*Cellana toreuma* (Reeve)	Yomegakasa	Pl. 1, Fig. 1
			Cellana grata (Gould)	Bekkougasa	Pl. 1, Fig. 2
			Cellana orientalis (Pilsbry)	Kurumagasa	Pl. 1, Fig. 3
		Lottiidae	*Patelloida lanx* (Reeve)	Unoashi	Pl. 1, Fig. 4
			Patelloida pygmaea (Dunker)	Himekozara	Pl. 1, Fig. 5
			Lottia dorsuosa (Gould)	Kamogai	Pl. 1, Fig. 6
			Lottia tenuisculpta Sasaki and Okutani	Komorebikogamogai	Pl. 1, Fig. 7
	Vetigastropoda	Trochidae	*Umbonium costatum* (Valenciennes)	Kisago	Pl. 2, Fig. 1
		Turbinidae	*Turbo* (*Batillus*) *cornutus* Lightfoot	Sazae	Pl. 2, Fig. 2
		Tegulidae	*Chlorostoma lischkei* Tapparone-Canefri	Kubogai	Pl. 2, Fig. 3
			Chlorostoma turbinatum A. Adams	Hesoakikubogai	Pl. 2, Fig. 4
		Fissurellidae	*Tugali decussata* A. Adams	Shirosusokakegai	Pl. 2, Fig. 5
	Caenogastropoda	Cerithiidae	*Rhinoclavis kochi* (Philippi)	Kanimorigai	Pl. 2, Fig. 6
		Hipponicidae	*Sabia conicus* (Schumacher)	Kikusuzume	Pl. 2, Fig. 7
		Eulimidae	*Eulima bifascialis* (A. Adams)	Hanagouna	Pl. 2, Fig. 8
		Strombidae	*Strombus* (*Doxander*) *japonicus* Reeve	Shidorogai	Pl. 2, Fig. 9
		Calyptraeidae	*Crepidula* (*Bostrycapulus*) *gravispinosus* (Kuroda and Habe)	Awabunegai	Pl. 2, Fig. 10
		Vermetidae	*Thylacodes adamsii* (Mörch)	Oohebigai	Pl. 2, Fig. 11
		Naticidae	*Glossaulax didyma* (Röding)	Tsumetagai	Pl. 3, Fig. 1
		Cassidae	*Phalium flammiferum* (Röding)	Kazuragai	Pl. 3, Fig. 2
		Tonnidae	*Tonna lischkeana* (Küster)	Uzuramiyashirogai	Pl. 3, Fig. 3
		Epitoniidae	*Epitonium auritum* (G.B. Sowerby II)	Odamaki	Pl. 3, Fig. 4
		Janthinidae	*Janthina globosa* Swainson	Rurigai	Pl. 3, Fig. 5
		Columbellidae	*Mitrella bicincta* (Gould)	Mugigai	Pl. 3, Fig. 6
		Nassariidae	*Nassarius conoidalis* (Deshayes)	Araregai	Pl. 3, Fig. 7
			Nassarius (*Niotha*) *livescens* (Philippi)	Mushirogai	Pl. 3, Fig. 8
		Fasciolariidae	*Fusinus perplexus* (A. Adams)	Naganishi	Pl. 4, Fig. 1
		Babyloniidae	*Babylonia japonica* (Reeve)	Bai	Pl. 4, Fig. 2
		Muricidae	*Reishia bronni* (Dunker)	Reishigai	Pl. 4, Fig. 3
			Reishia clavigera (Küster)	Ibonishi	Pl. 4, Fig. 4
		Olivellidae	*Olivella fulgurata* (Adams and Reeve)	Mushibotaru	Pl. 4, Fig. 5
		Olividae	*Oliva mustelina* Lamarck	Makuragai	Pl. 4, Fig. 6
		Cancellariidae	*Momoebora sinensis* (Reeve)	Momoebora	Pl. 4, Fig. 7
			Sydaphera spengleriana (Deshayes)	Koromogai	Pl. 4, Fig. 8
			Cancellaria (*Habesolatia*) *nodulifera* G.B. Sowerby I	Tokashioriire	Pl. 4, Fig. 9
	Euopisthobranchia	Philinidae	*Philine argentata* Gould	Kisewatagai	Pl. 4, Fig. 10
	Mesogastropoda	Viviparidae	*Cipangopaludina japonica* (Martens)	Ootanishi	Pl. 15, Fig. 1
			Sinotaia quadrata histrica (Gould)	Himetanishi	Pl. 15, Fig. 2
		Pleuroceridae	*Semisulcospira libertina* (Gould)	Kawanina	Pl. 15, Fig. 3
	Bassommatophora	Physidae	*Physella acuta* Draparnaud	Sakamakigai	Pl. 15, Fig. 4
Cephalopoda	Octopoda	Argonautidae	*Argonauta argo* Linnaeus	Aoigai	Pl. 5, Fig. 1
	Sepioida	Sepiidae	*Acanthosepion esculenta* (Hoyle)	Kouika	Pl. 5, Fig. 2
			Doratosepion kobiensis (Hoyle)	Himekouika	Pl. 5, Fig. 3
Scaphopoda	Dentaliida	Gadilinidae	*Compressidens kikuchii* (Kuroda and Habe)	Hinatsunogai	Pl. 5, Fig. 4
	Gadilida	Gadilidae	*Siphonodentalium isaotakii* Habe	Kuchikiretsunogai	Pl. 5, Fig. 5
Bivalvia	Nuculanoida	Nuculanidae	*Nuculana* (*Saccella*) *sematensis* (Suzuki and Ishizuka)	Arasujisodegai	Pl. 6, Fig. 1
	Arcoida	Arcidae	*Arca boucardi* Jousseaume	Koberutofunegai	Pl. 6, Fig. 2
			Barbatia (*Ustularca*) *stearnsii* (Pilsbry)	Hanaegai	Pl. 6, Fig. 3
			Scapharca inaequivalvis (Bruguière)	Kuichigaisarubou	Pl. 6, Fig. 4
			Scapharca satowi (Dunker)	Satougai	Pl. 6, Fig. 5
		Parallelodontidae	*Porterius dalli* (E.A. Smith)	Shikoroegai	Pl. 6, Fig. 6
		Noetiidae	*Arcopsis symmetrica* (Reeve)	Mimiegai	Pl. 6, Fig. 7
		Glycymerididae	*Glycymeris* (*Veletuceta*) *albolineata* (Lischke)	Benkeigai	Pl. 6, Fig. 8
	Mytiloida	Mytilidae	*Mytilus galloprovincialis* Lamrck	Murasakiigai	Pl. 7, Fig. 1
			Mytilus coruscus Gould	Igai	Pl. 7, Fig. 2
			Septifer virgatus (Wiegmann)	Murasakiinko	Pl. 7, Fig. 3
			Septifer keenae Nomura	Himeigai	Pl. 7, Fig. 4
			Modiolus nipponicus (Oyama)	Hibarigai	Pl. 7, Fig. 5
			Gregariella barbata (Gmelin)	Chijimitamaegai	Pl. 7, Fig. 6
	Pterioida	Ostreidae	*Crassostrea gigas* (Thunberg)	Magaki	Pl. 7, Fig. 7
			Crossostrea nippona (Seki)	Iwagaki	Pl. 7, Fig. 8

Class	Oder	Family	Species	Japanese name	Plate and figure number
	Limoida	Limidae	*Limaria hakodatensis* (Tokunaga)	Fukureyukimino	Pl. 8, Fig. 1
	Pectinoida	Pectinidae	*Chlamys* (*Azumapecten*) *farreri nipponensis* Kuroda	Azumanishiki	Pl. 8, Fig. 2
			Swiftopecten swiftii (Bernardi)	Ezokinchaku	Pl. 8, Fig. 3
			Pecten albicans (Schröter)	Itayagai	Pl. 8, Fig. 4
		Spondylidae	*Spondylus cruentus* Lischke	Chiribotan	Pl. 8, Fig. 5
		Anomiidae	*Anomia chinensis* Philippi	Namimagashiwa	Pl. 8, Fig. 6
			Monia macroschisma (Deshayes)	Namimagashiwamodoki	Pl. 8, Fig. 7
	Carditoida	Carditidae	*Cardita leana* Dunker	Tomayagai	Pl. 9, Fig. 1
	Anomalodesmata	Lyonsiidae	*Agriodesma navicula* (A. Adams and Reeve)	Obikui	Pl. 9, Fig. 2
		Laternulidae	*Laternula anatina* (Linnaeus)	Okinagai	Pl. 9, Fig. 3
	Veneroida	Lucinidae	*Epicodakia delicatula* (Pilsbry)	Umiasagai	Pl. 9, Fig. 4
		Ungulinidae	*Joannisiella nomurai* (Habe)	Hirashiogama	Pl. 9, Fig. 5
			Joannisiella tsuchii (Yamamoto and Habe)	Atsushiogama	Pl. 9, Fig. 6
		Chamidae	*Chama japonica* Lamarck	Kikuzaru	Pl. 9, Fig. 7
		Lasaeidae	*Kellia porculus* Pilsbry	Kohakunotsuyu	Pl. 9, Fig. 8
		Sportellidae	*Basterotia stimpsoni* (A. Adams)	Soyokazegai	Pl. 9, Fig. 9
		Trapezidae	*Coralliophaga coralliophaga* (Gmelin)	Tagasodegai	Pl. 9, Fig. 10
			Trapezium liratum (Reeve)	Unenashitomayagai	Pl. 9, Fig. 11
		Corbiculidae	*Corbicula japonica* Prime	Yamatoshijimi	Pl. 9, Fig. 12
		Cardiidae	*Fulvia mutica* (Reeve)	Torigai	Pl. 10, Fig. 1
		Veneridae	*Placamen foliaceum* (Philippi)	Hanagai	Pl. 10, Fig. 2
			Protothaca jedoensis (Lischke)	Oniasari	Pl. 10, Fig. 3
			Pitar japonicus Kuroda and Kawamoto	Usuhamaguri	Pl. 10, Fig. 4
			Phacosoma troscheli (Lischke)	Maruhinagai	Pl. 10, Fig. 5
			Ruditapes philippinarum (A. Adams and Reeve)	Asari	Pl. 10, Fig. 6
			Paphia amabilis (Philippi)	Satsumaakagai	Pl. 10, Fig. 7
			Irus mitis (Deshayes)	Matsukazegai	Pl. 10, Fig. 8
			Irus macrophyllus (Deshayes)	Hanematsukaze	Pl. 10, Fig. 9
			Irus ishibashianus (Kira)	Okinamatsukaze	Pl. 10, Fig. 10
			Macridiscus melanaegis (Römer)	Kotamagai	Pl. 10, Fig. 11
			Callista chinensis (Holten)	Matsuyamawasure	Pl. 10, Fig. 12
			Meretrix lamarckii Deshayes	Chousenhamaguri	Pl. 11, Fig. 1
			Meretrix petechialis (Lamarck)	Shinahamaguri	Pl. 11, Fig. 2
			Clementia vatheleti Mabille	Fusumagai	Pl. 11, Fig. 3
		Petricolidae	*Petricolirus aequistriatus* (G.B. Sowerby)	Shiotsugai	Pl. 11, Fig. 4
		Donacidae	*Chion semigranosa* (Dunker)	Fujinohanagai	Pl. 11, Fig. 5
			Latona cuneata (Linnaeus)	Naminokogai	Pl. 11, Fig. 6
		Tellinidae	*Pharaonella sieboldii* (Deshayes)	Benigai	Pl. 11, Fig. 7
			Tellinides ovalis (G.B. Sowerby I)	Hirazakura	Pl. 11, Fig. 8
			Megangulus zyonoensis (Hatai and Nisiyama)	Arasujisaragai	Pl. 11, Fig. 9
			Nitidotellina iridella (Martens)	Kabazakura	Pl. 11, Fig. 10
			Macoma praetexta (Martens)	Oomomonohana	Pl. 11, Fig. 11
			Macoma sectior Oyama	Sagigai	Pl. 12, Fig. 1
			Heteromacoma irus oyamai Kira	Marushiratorimodoki	Pl. 12, Fig. 2
		Psammobiidae	*Soletellina boeddinghausi* Lischke	Fujinamigai	Pl. 12, Fig. 3
			Nuttallia japonica (Reeve)	Isoshijimi	Pl. 12, Fig. 4
		Solecurtidae	*Solecurtus divaricatus* (Lischke)	Kinutaagemaki	Pl. 12, Fig. 5
		Solenidae	*Solen strictus* Gould	Mategai	Pl. 12, Fig. 6
			Solen kurodai Habe	Dandaramategai	Pl. 12, Fig. 7
		Cultellidae	*Siliqua pulchella* (Dunker)	Mizogai	Pl. 12, Fig. 8
		Mactridae	*Mactra chinensis* Philippi	Bakagai	Pl. 13, Fig. 1
			Coelomactra antiquata (Spengler)	Arisogai	Pl. 13, Fig. 2
			Pseudocardium sachalinense (Schrenck)	Ubagai	Pl. 13, Fig. 3
			Lutraria maxima Jonas	Ootorigai	Pl. 13, Fig. 4
			Raetellops pulchellus (A. Adams and Reeve)	Chiyonohanagai	Pl. 13, Fig. 5
	Myoida	Cardiliidae	*Cardilia semisulcata* (Lamarck)	Kisagai	Pl. 13, Fig. 6
		Corbulidae	*Solidicorbula erythrodon* (Lamarck)	Kuchibenigai	Pl. 13, Fig. 7
		Pholadidae	*Penitella* sp.	Kamomegai	Pl. 14, Fig. 1
			Zirfaea constricta (G.B. Sowerby)	Niogaimodoki	Pl. 14, Fig. 2
			Barnea (*Anchomasa*) *fragilis* (G.B. Sowerby)	Niogai	Pl. 14, Fig. 3
			Barnea (*Umitakea*) *japonica* (Yokoyama)	Umitake	Pl. 14, Fig. 4
	Unionoida	Unionidae	*Sinohyriopsis schlegelii* (Martens)	Ikechougai	Pl. 15, Fig. 5

Results and discussion

Examining the collected molluscan shells, we identified a total of 123 species, consisting of 40 gastropods, 3 cephalopods, 2 scaphopods and 78 bivalves (Table 1, Plates 1–15). According to Amano (2001), the molluscan fauna washed up on the coasts of four sites in Joetsu, Niigata, 90 km southwest of Ikarashi beach, included 126 species. Such a similarity in the number of species may suggest that the present collection reflects the shallow molluscan fauna available from beachcombing sampling.

The molluscan shells included five freshwater species, *Cipangopaludina japonica* (Martens), *Sinotaia quadrata histrica* (Gould), *Semisulcospira libertina* (Gould), *Physella acuta* Draparnaud and *Hyriopsis schlegelii* (Martens) (Plate 15). Given that the Chinese pond turtle *Mauremys reevesii* (Gray) washed up on the beach, the shells of freshwater species indicate to have been transported via the Shin-kawa River near the present beachcombing site (Fig. 1).

Among the present marine molluscs, common species on Ikarashi beach are *Scapharca inaequivalvis* (Bruguière), *Mactra chinensis* Philippi, *Macridiscus melanaegis* (Römer) and *Chion semigranosa* (Dunker). The latter two are the most abundant living species on the sandy shore around Ikarashi beach (Takada et al., 2015) and seem to be para-autochthonous elements for the present beachcombing.

Well-preserved shells of *Corbicula japonica* Prime, *Ruditapes philippinarum* (A. Adams and Reeve), *Nuttallia japonica* (Reeve) and *Solen strictus* Gould frequently washed up around the wharf. These species are known to inhabit shallow, calm benthic conditions such as inner bays and estuaries (Okutani, 2017), which could be present in the Shin-kawa Fishing Port, as it is surrounded by wharfs. On the wharf, we recognised the presence of *Crassostrea nippona* (Seki), but not *Crassostrea gigas* (Thunberg) or *Neopycnodonte cochlear* (Poli). Because all the shells of *C. gigas* and *N. cochlear* were solitary on the beach even if they were far from the wharf, both species may adapt to deeper hard substrates such as tetrapod blocks and gravels under the shallow sea, which we cannot observe during beachcombing.

The holoplanktonic gastropod *Janthina globosa* Swainson, the pelagic octopus *Argonauta argo* Linnaeus and the cuttlefish *Acanthosepion esculenta* (Hoyle) originate in temperate seas (Okutani, 2017), and can drift along with the Tsushima Warm Current, as is observed in the case of planktonic animals (e.g., Matsuoka et al., 2001, 2002; Itaki, 2003; Itaki et al., 2003; Kurihara et al., 2006, 2007, 2008; Kurihara and Matsuoka, 2009, 2010). The benthic molluscan fauna includes both cool and warm water species, e.g., cool water for *Megangulus zyonoensis* (Hatai and Nisiyama) and warm water for *Tellinides ovalis* (G. B. Sowerby I) (Amano, 2001). Previous studies have shown that the ratio of both types of species varies from south to north due to the influence of seawater temperature (Amano, 2001; Takebayashi and Wada, 2010). Furthermore, the distributions of some benthic animals appear to expand northward along the coast of the Sea of Japan (e.g., Gallagher et al., 2015; Yoshioka, 2020), which seems to reflect climatic changes. Based on these biogeographic findings, episodic reports of molluscan fauna washing up on beaches may help us to understand the environmental changes in the Sea of Japan (e.g., Enya and Suzuki, 2020), contributing to Sustainable Development Goal 13: climate action.

Acknowledgements

We gratefully acknowledge Hiroshi Kurita (Niigata University) for helpful support of experimental facilities. We also express sincere thanks to Taro Yoshimura (The University of Tokyo) and Takenori Sasaki (The University of Tokyo) for identification of molluscan shells in part. We thank reviewer, Yosuke Ibaraki (Fossa Magna Museum). The specimen preparation and curation were financially supported in part by the JSPS KAKENHI Grant Numbers 20K04147 and 22K03795. This study was a collaborative research activity of the "Frontier Study Project" in the Faculty of Science, Niigata University, and of the Human Resource Development Program on Field Science Research in the Indo-Pacific Region, which has received endorsement from the Ministry of Education, Culture, Sports, Science and Technology (MEXT) as part of FY2022 Inter University Exchange Project.

References

Amano, K., 2001, Development of teaching material for deeply understanding the environmental changes—By the comparison between the recent and fossil molluscs—. *Educat. Earth Sci.*, **54**, 225–236.

Davies, L., Kemp, A., O'Loughlin, C. and Korczynskyj, D., 2022, Is conscientious beachcombing the key to 'unlock' marine plastic pollution trends through citizen science? A case study from Cockburn Sound, Western Australia. *Mar. Pollut. Bull.*, **177**, 113519.

Desa, U. N., 2016, *Transforming our world: The 2030 Agenda for Sustainable Development*, 35p.

Donovan, S. K., 2011, Beachcombing and palaeoecology. *Geol. Today*, **27**, 25–33.

Enya, T. and Suzuki, A., 2020, Molluscs drifted on the coast of Okushiri Island, Hokkaido, Japan. *Jour. Jap. Drif. Soc.*, **18**, 19–25 (in Japanese with English abstract).

Gallagher, S. J., Kitamura, A., Iryu, Y., Itaki, T., Koizumi, I. and Hoiles, P. W., 2015, The Pliocene to recent history of the Kuroshio and Tsushima Currents: a multi-proxy approach. *Prog. Earth Planet. Sci.*, **2**, article number 17.

Ishizaki, Y., Ogura, M., Takahashi, C., Kaneko, M., Imura, A. and Shiino, Y., 2023, Burrow morphology of ghost crab *Ocypode stimpsoni* on Ikarashi beach, Niigata, Japan. *Plankton Benthos Res.*, **18**, 1–12.

Ishizaki, Y. and Shiino, Y., 2023, A discinid shell on Ikarashi beach, Niigata, Japan. *Sci. Rep., Niigata Univ. (Geol.)*, no. 38, 1–16.

Itaki, T., 2003, Depth-related radiolarian assemblage in the water column and surface sediments of the Japan Sea. *Marine Micropaleontol.*, **47**, 253–270.

Itaki, T., Matsuoka, A., Yoshida, K., Machidori, S., Shinzawa, M. and Todo, T., 2003, Late spring radiolarian fauna in the surface water off Tassha, Aikawa Town, Sado, central Japan. *Sci. Rep., Niigata Univ. Ser. E (Geol.)*, no. 18, 41–51.

Kurihara, T. and Matsuoka, A., 2009, A late-winter (March 10, 2008) living radiolarian fauna in surface–subsurface waters of the Japan Sea off Tassha, Sado Island, central Japan. *Sci. Rep., Niigata Univ. (Geol.)*, no. 24, 81–90.

Kurihara, T. and Matsuoka, A., 2010, Living radiolarian fauna of late autumn (November 13, 2008) in surface–subsurface waters of the Japan Sea off Tassha, Sado Island, central Japan. *Sci. Rep., Niigata Univ. (Geol.)*, no. 25, 83–92.

Kurihara, T., Shimotani, T. and Matsuoka, A., 2006, Water temperature, salinity, algalchlorophyll profiles and radiolarian fauna in the surface and subsurface waters in early June, off Tassha, Sado Island, central Japan. *Sci. Rep., Niigata Univ. (Geol.)*, no. 21, 31–46.

Kurihara, T., Uchida, K., Shimotani, T. and Matsuoka, A., 2007, Radiolarian faunas and water properties in surface and subsurface waters of the Japan Sea in September 2005, off Tassha, Sado Island, central Japan. *Sci. Rep., Niigata Univ. (Geol.)*, no. 22, 43–56.

Kurihara, T., Uchida, K., Shimotani, T. and Matsuoka, A., 2008, Radiolarian faunal characteristics in surface–subsurface waters of the Japan Sea off Tassha, Sado Island, central Japan in June 2007: inflowing radiolarians on the Tsushima Warm Current. *Sci. Rep., Niigata Univ. (Geol.)*, no. 23, 65–74.

Matsuoka, A., Shinzawa, M., Yoshida, K., Machidori, S., Kurita, H. and Todo, T., 2002, Early summer radiolarian fauna in surface waters off Tassha, Aikawa Town, Sado Island, central Japan. *Sci. Rep., Niigata Univ. Ser. E (Geol.)*, no. 17, 17–25.

Matsuoka, A., Yoshida, K., Hasegawa, S., Shinzawa, M., Tamura, K., Sakumoto, T., Yabe, H., Niikawa, I. and Tateishi, M., 2001, Temperature profile and radiolarian fauna in surface waters off Tassha, Aikawa Town, Sado Island, central Japan. *Sci. Rep., Niigata Univ. Ser. E (Geol.)*, no. 16, 83–93.

Okutani, T., 2004, *Encyclopedia of Shellfish*. Sekaibunkasha, Tokyo, 399 pp. (in Japanese).

Okutani, T., 2017, *Marine Mollusks in Japan. The Second Edition*. 1375 pp. Tokai University Press, Hiratsuka (in Japanese with English explanation).

Seo, T. and Tanangonan, J., 2014, Recent marine malacofauna in Kagawa Prefecture. *Mem. Fac. Agric. Kinki Univ.*, **47**, 87–124 (in Japanese).

Takada, Y., Kajihara, N., Abe, S., Iseki, T., Yagi, Y., Sawada, H., Saito, H., Mochizuki, S. and Murakami, T., 2015, Distribution of *Donax semigranosus* and other bivalves on sandy shore swash zones along the Japan Sea coast of Honshu. *Venus*, **73**, 51–64.

Takagi, Y., 1992, Distribution and ecology of molluscs in Echigo Nanaura Coast, specifically addressing the case of *Nodilittorina radiata*. *Res. Rep. Niigata Pref. Educ. Center*, no. 137, 45–52 (in Japanese). *

Takebayashi, Y. and Wada, T., 2010, Mollusks drifted on the sandy beaches in eastern part of Tottori Prefecture, Honshu, Japan: with online publication of the web book. *Bull. Tottori Prefectural Mus.*, **47**, 7–25 (in Japanese with English abstract).

Yoshioka, T., 2016, Beached shells of *Discradisca* (Brachiopoda) in Hokuriku along the coast of the Japan Sea. *Jour. Jap. Drif. Soc.*, **14**, 39–40 (in Japanese).

Yoshioka, T., 2020, Mass stranding of discinid brachiopod shells related to artificial habitat disturbance. *Jour. Jap. Drif. Soc.*, **18**, 13–18 (in Japanese).

*English translation from the original written in Japanese

Explanation of Plate 1
Patellogastropoda (JN: Japanese name).
Fig. 1. *Cellana toreuma* (Reeve). JN: Yomegakasa.
Fig. 2. *Cellana grata* (Gould). JN: Bekkougasa.
Fig. 3. *Cellana orientalis* (Pilsbry). JN: Kurumagasa.
Fig. 4. *Patelloida lanx* (Reeve). JN: Unoashi.
Fig. 5. *Patelloida pygmaea* (Dunker). JN: Himekozara.
Fig. 6. *Lottia dorsuosa* (Gould). JN: Kamogai.
Fig. 7. *Lottia tenuisculpta* Sasaki and Okutani. JN: Komorebikogamogai.

Explanation of Plate 2
Vetigastropoda and Caenogastropoda (JN: Japanese name).
Fig. 1. *Umbonium costatum* (Valenciennes). JN: Kisago.
Fig. 2. *Turbo* (*Batillus*) *cornutus* Lightfoot. JN: Sazae.
Fig. 3. *Chlorostoma lischkei* Tapparone-Canefri. JN: Kubogai.
Fig. 4. *Chlorostoma turbinatum* A. Adams. JN: Hesoakikubogai.
Fig. 5. *Tugali decussata* A. Adams. JN: Shirosusokakegai.
Fig. 6. *Rhinoclavis kochi* (Philippi). JN: Kanimorigai.
Fig. 7. *Sabia conicus* (Schumacher). JN: Kikusuzume.
Fig. 8. *Eulima bifascialis* (A. Adams). JN: Hanagouna.
Fig. 9. *Strombus* (*Doxander*) *japonicus* Reeve. JN: Shidorogai.
Fig. 10. *Crepidula* (*Bostrycapulus*) *gravispinosus* (Kuroda and Habe). JN: Awabunegai.
Fig. 11. *Thylacodes adamsii* (Mörch). JN: Oohebigai.

Explanation of Plate 3
Caenogastropoda (JN: Japanese name).
Fig. 1. *Glossaulax didyma* (Röding). JN: Tsumetagai.
Fig. 2. *Phalium flammiferum* (Röding). JN: Kazuragai.
Fig. 3. *Tonna lischkeana* (Küster). JN: Uzuramiyashirogai.
Fig. 4. *Epitonium auritum* (G.B. Sowerby II). JN: Odamaki.
Fig. 5. *Janthina globosa* Swainson. JN: Rurigai.
Fig. 6. *Mitrella bicincta* (Gould). JN: Mugigai.
Fig. 7. *Nassarius conoidalis* (Deshayes). JN: Araregai.
Fig. 8. *Nassarius* (*Niotha*) *livescens* (Philippi). JN: Mushirogai.

Explanation of Plate 4
Caenogastropoda and Euopisthobranchia (JN: Japanese name).
Fig. 1. *Fusinus perplexus* (A. Adams). JN: Naganishi.
Fig. 2. *Babylonia japonica* (Reeve). JN: Bai.
Fig. 3. *Reishia bronni* (Dunker). JN: Reishigai.
Fig. 4. *Reishia clavigera* (Küster). JN: Ibonishi.
Fig. 5. *Olivella fulgurata* (Adams and Reeve). JN: Mushibotaru.
Fig. 6. *Oliva mustelina* Lamarck. JN: Makuragai.
Fig. 7. *Momoebora sinensis* (Reeve). JN: Momoebora.
Fig. 8. *Sydaphera spengleriana* (Deshayes). JN: Koromogai.
Fig. 9. *Cancellaria* (*Habesolatia*) *nodulifera* G.B. Sowerby I. JN: Tokashioriire.
Fig. 10. *Philine argentata* Gould. JN: Kisewatagai.

Explanation of Plate 5
Cephalopoda and Scaphopoda (JN: Japanese name).
Fig. 1. *Argonauta argo* Linnaeus. JN: Aoigai.
Fig. 2. *Acanthosepion esculenta* (Hoyle). JN: Kouika.
Fig. 3. *Doratosepion kobiensis* (Hoyle). JN: Himekouika.
Fig. 4. *Compressidens kikuchii* (Kuroda and Habe). JN: Hinatsunogai.
Fig. 5. *Siphonodentalium isaotakii* Habe. JN: Kuchikiretsunogai.

Explanation of Plate 6

Nuculanoida and Arcoida (JN: Japanese name).
Fig. 1. *Nuculana* (*Saccella*) *sematensis* (Suzuki and Ishizuka). JN: Arasujisodegai.
Fig. 2. *Arca boucardi* Jousseaume. JN: Koberutofunegai.
Fig. 3. *Barbatia* (*Ustularca*) *stearnsii* (Pilsbry). JN: Hanaegai.
Fig. 4. *Scapharca inaequivalvis* (Bruguière). JN: Kuichigaisarubou.
Fig. 5. *Scapharca satowi* (Dunker). JN: Satougai.
Fig. 6. *Porterius dalli* (E.A. Smith). JN: Shikoroegai.
Fig. 7. *Arcopsis symmetrica* (Reeve). JN: Mimiegai.
Fig. 8. *Glycymeris* (*Veletuceta*) *albolineata* (Lischke). JN: Benkeigai.

Explanation of Plate 7

Mytiloida and Pterioida (JN: Japanese name).
Fig. 1. *Mytilus galloprovincialis* Lamrck. JN: Murasakiigai.
Fig. 2. *Mytilus coruscus* Gould. JN: Igai.
Fig. 3. *Septifer virgatus* (Wiegmann). JN: Murasakiinko.
Fig. 4. *Septifer keenae* Nomura. JN: Himeigai.
Fig. 5. *Modiolus nipponicus* (Oyama). JN: Hibarigai.
Fig. 6. *Gregariella barbata* (Gmelin). JN: Chijimitamaegai.
Fig. 7. *Crassostrea gigas* (Thunberg). JN: Magaki.
Fig. 8. *Crossostrea nippona* (Seki). JN: Iwagaki.

Explanation of Plate 8

Limoida and Pectinoida (JN: Japanese name).
Fig. 1. *Limaria hakodatensis* (Tokunaga). JN: Fukureyukimino.
Fig. 2. *Chlamys* (*Azumapecten*) *farreri nipponensis* Kuroda. JN: Azumanishiki.
Fig. 3. *Swiftopecten swiftii* (Bernardi). JN: Ezokinchaku.
Fig. 4. *Pecten albicans* (Schröter). JN: Itayagai.
Fig. 5. *Spondylus cruentus* Lischke. JN: Chiribotan.
Fig. 6. *Anomia chinensis* Philippi. JN: Namimagashiwa.
Fig. 7. *Monia macroschisma* (Deshayes). JN: Namimagashiwamodoki.

Explanation of Plate 9

Veneroida (JN: Japanese name).
Fig. 1. *Cardita leana* Dunker. JN: Tomayagai.
Fig. 2. *Agriodesma navicula* (A. Adams and Reeve). JN: Obikui.
Fig. 3. *Laternula anatina* (Linnaeus). JN: Okinagai.
Fig. 4. *Epicodakia delicatula* (Pilsbry). JN: Umiasagai.
Fig. 5. *Joannisiella nomurai* (Habe). JN: Hirashiogama.
Fig. 6. *Joannisiella tsuchii* (Yamamoto and Habe). JN: Atsushiogama.
Fig. 7. *Chama japonica* Lamarck. JN: Kikuzaru.
Fig. 8. *Kellia porculus* Pilsbry. JN: Kohakunotsuyu.
Fig. 9. *Basterotia stimpsoni* (A. Adams). JN: Soyokazegai
Fig. 10. *Coralliophaga coralliophaga* (Gmelin). JN: Tagasodegai.
Fig. 11. *Trapezium liratum* (Reeve). JN: Unenashitomayagai.
Fig. 12. *Corbicula japonica* Prime. JN: Yamatoshijimi.

Explanation of Plate 10

Veneroida (JN: Japanese name).
Fig. 1. *Fulvia mutica* (Reeve). JN: Torigai.
Fig. 2. *Placamen foliaceum* (Philippi). JN: Hanagai.
Fig. 3. *Protothaca jedoensis* (Lischke). JN: Oniasari.
Fig. 4. *Pitar japonicus* Kuroda and Kawamoto. JN: Usuhamaguri.
Fig. 5. *Phacosoma troscheli* (Lischke). JN: Maruhinagai.
Fig. 6. *Ruditapes philippinarum* (A. Adams and Reeve). JN: Asari.

Fig. 7. *Paphia amabilis* (Philippi). JN: Satsumaakagai.
Fig. 8. *Irus mitis* (Deshayes). JN: Matsukazegai.
Fig. 9. *Irus macrophyllus* (Deshayes). JN: Hanematsukaze.
Fig. 10. *Irus ishibashianus* (Kira). JN: Okinamatsukaze.
Fig. 11. *Macridiscus melanaegis* (Römer). JN: Kotamagai.
Fig. 12. *Callista chinensis* (Holten). JN: Matsuyamawasure.

Explanation of Plate 11
Veneroida (JN: Japanese name).
Fig. 1. *Meretrix lamarckii* Deshayes. JN: Chousenhamaguri.
Fig. 2. *Meretrix petechialis* (Lamarck). JN: Shinahamaguri.
Fig. 3. *Clementia vatheleti* Mabille. JN: Fusumagai.
Fig. 4. *Petricolirus aequistriatus* (G.B. Sowerby). JN: Shiotsugai.
Fig. 5. *Chion semigranosa* (Dunker). JN: Fujinohanagai.
Fig. 6. *Latona cuneata* (Linnaeus). JN: Naminokogai.
Fig. 7. *Pharaonella sieboldii* (Deshayes). JN: Benigai.
Fig. 8. *Tellinides ovalis* (G.B. Sowerby I). JN: Hirazakura.
Fig. 9. *Megangulus zyonoensis* (Hatai and Nisiyama). JN: Arasujisaragai.
Fig. 10. *Nitidotellina iridella* (Martens). JN: Kabazakura.
Fig. 11. *Macoma praetexta* (Martens). JN: Oomomonohana.

Explanation of Plate 12
Veneroida (JN: Japanese name).
Fig. 1. *Macoma sectior* Oyama. JN: Sagigai.
Fig. 2. *Heteromacoma irus oyamai* Kira. JN: Marushiratorimodoki.
Fig. 3. *Soletellina boeddinghausi* Lischke. JN: Fujinamigai.
Fig. 4. *Nuttallia japonica* (Reeve). JN: Isoshijimi.
Fig. 5. *Solecurtus divaricatus* (Lischke). JN: Kinutaagemaki.
Fig. 6. *Solen strictus* Gould. JN: Mategai.
Fig. 7. *Solen kurodai* Habe. JN: Dandaramategai.
Fig. 8. *Siliqua pulchella* (Dunker). JN: Mizogai.

Explanation of Plate 13
Veneroida and Myoida (JN: Japanese name).
Fig. 1. *Mactra chinensis* Philippi. JN: Bakagai.
Fig. 2. *Coelomactra antiquata* (Spengler). JN: Arisogai.
Fig. 3. *Pseudocardium sachalinense* (Schrenck). JN: Ubagai.
Fig. 4. *Lutraria maxima* Jonas. JN: Ootorigai.
Fig. 5. *Raetellops pulchellus* (A. Adams and Reeve). JN: Chiyonohanagai.
Fig. 6. *Cardilia semisulcata* (Lamarck). JN: Kisagai.
Fig. 7. *Solidicorbula erythrodon* (Lamarck). JN: Kuchibenigai.

Explanation of Plate 14
Myoida (JN: Japanese name).
Fig. 1. *Penitella* sp. JN: Kamomegai.
Fig. 2. *Zirfaea constricta* (G.B. Sowerby). JN: Niogaimodoki.
Fig. 3. *Barnea* (*Anchomasa*) *fragilis* (G.B. Sowerby). JN: Niogai.
Fig. 4. *Barnea* (*Umitakea*) *japonica* (Yokoyama). JN: Umitake.

Explanation of Plate 15
Mesogastropoda, Bassommatophora and Unionoida (JN: Japanese name). Freshwater species.
Fig. 1. *Cipangopaludina japonica* (Martens). JN: Ootanishi.
Fig. 2. *Sinotaia quadrata histrica* (Gould). JN: Himetanishi.
Fig. 3. *Semisulcospira libertina* (Gould). JN: Kawanina.
Fig. 4. *Physella acuta* Draparnaud. JN: Sakamakigai.
Fig. 5. *Sinohyriopsis schlegelii* (Martens). JN: Ikechougai.

Plate 1

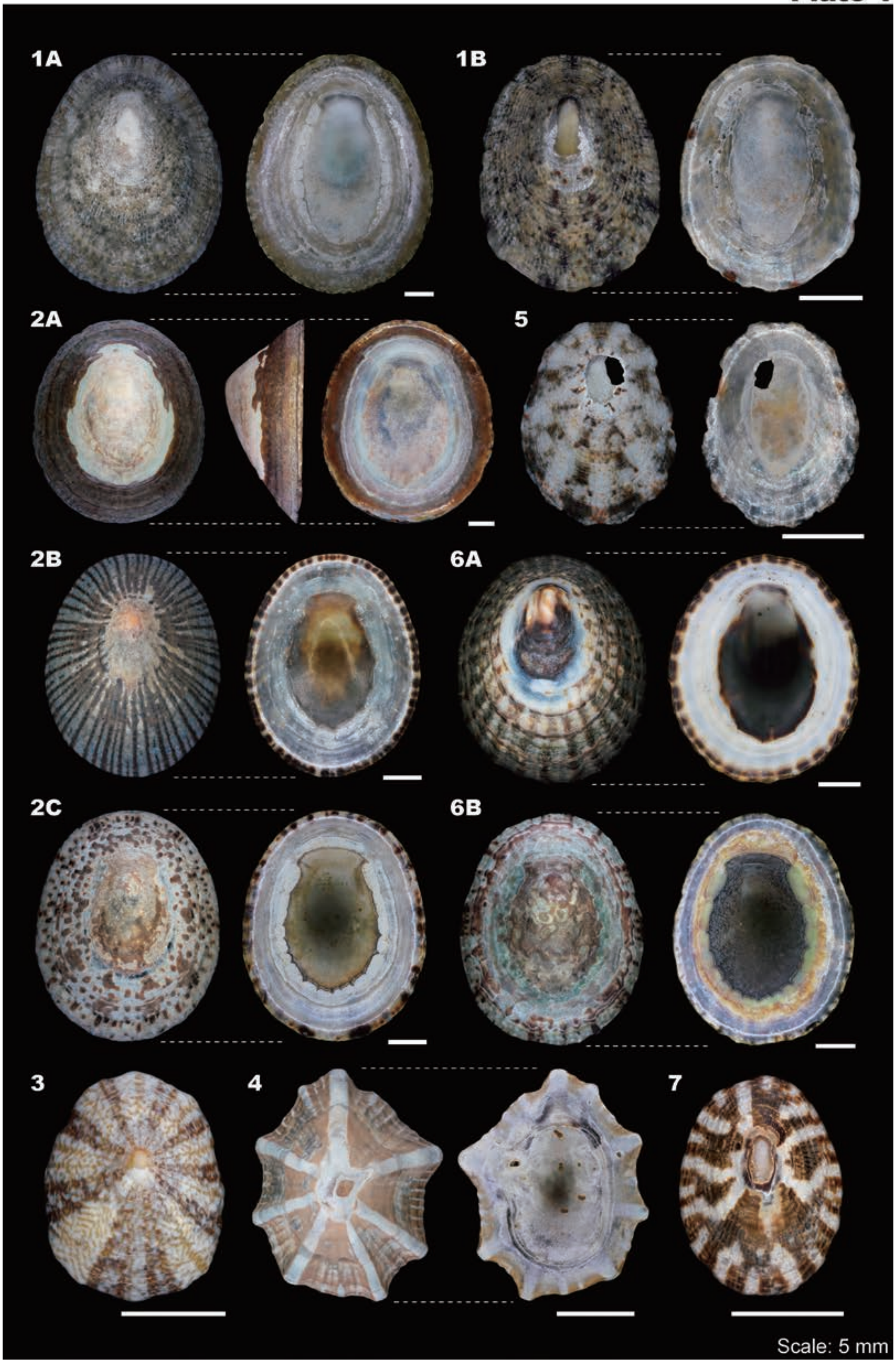

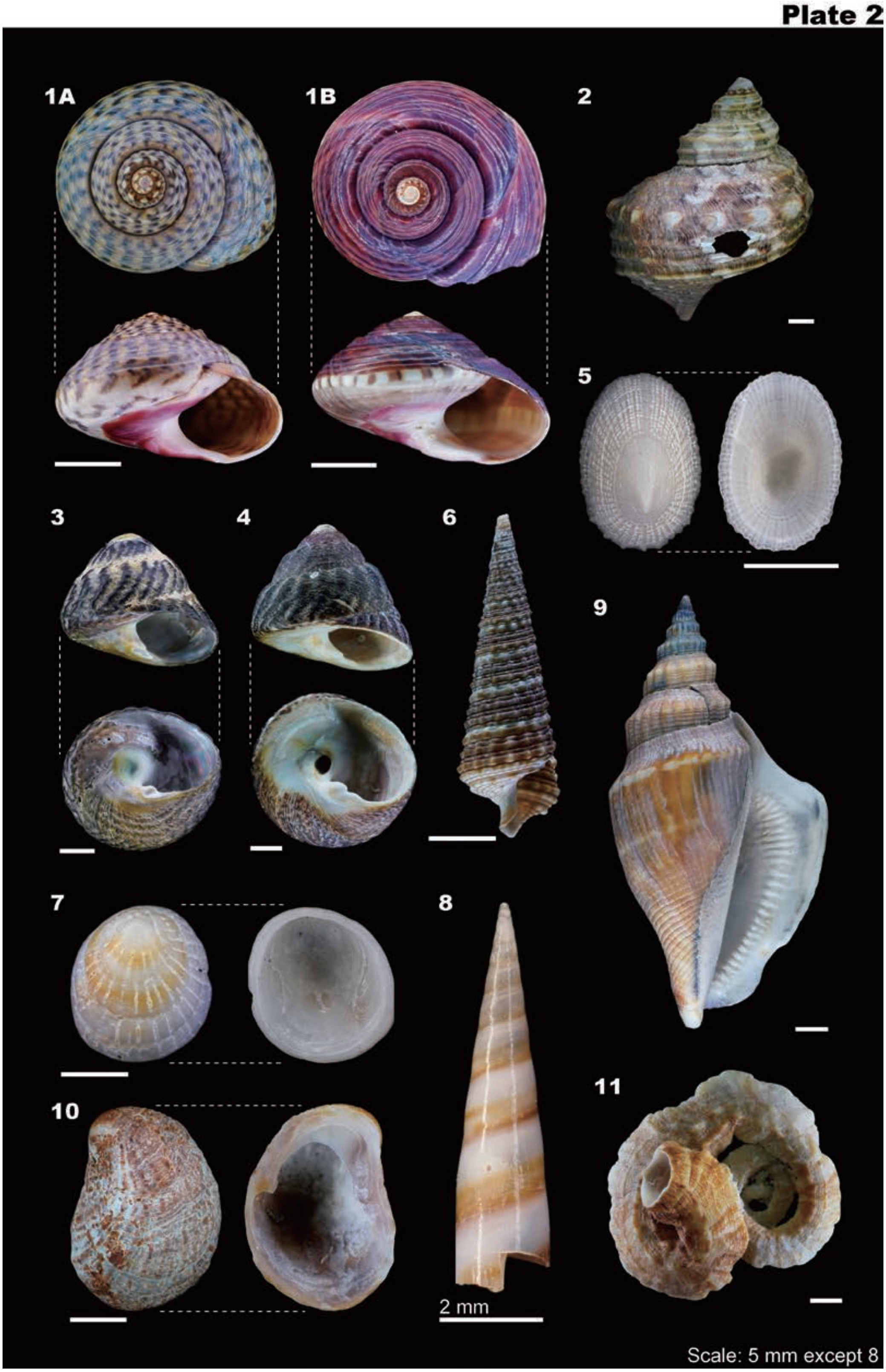
Plate 2
1A
1B
2
3
4
5
6
7
8
9
10
11
2 mm
Scale: 5 mm except 8

Plate 3

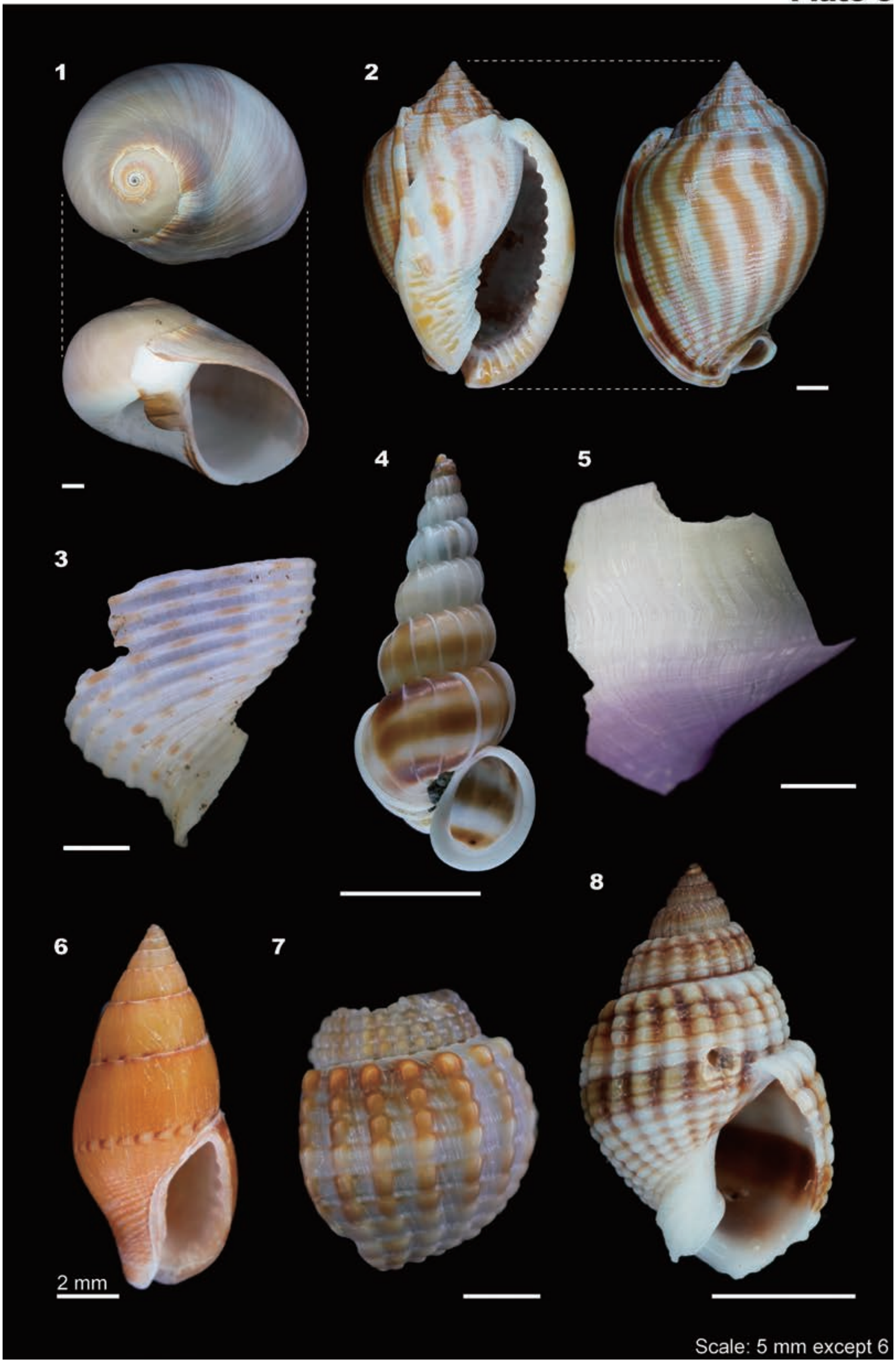

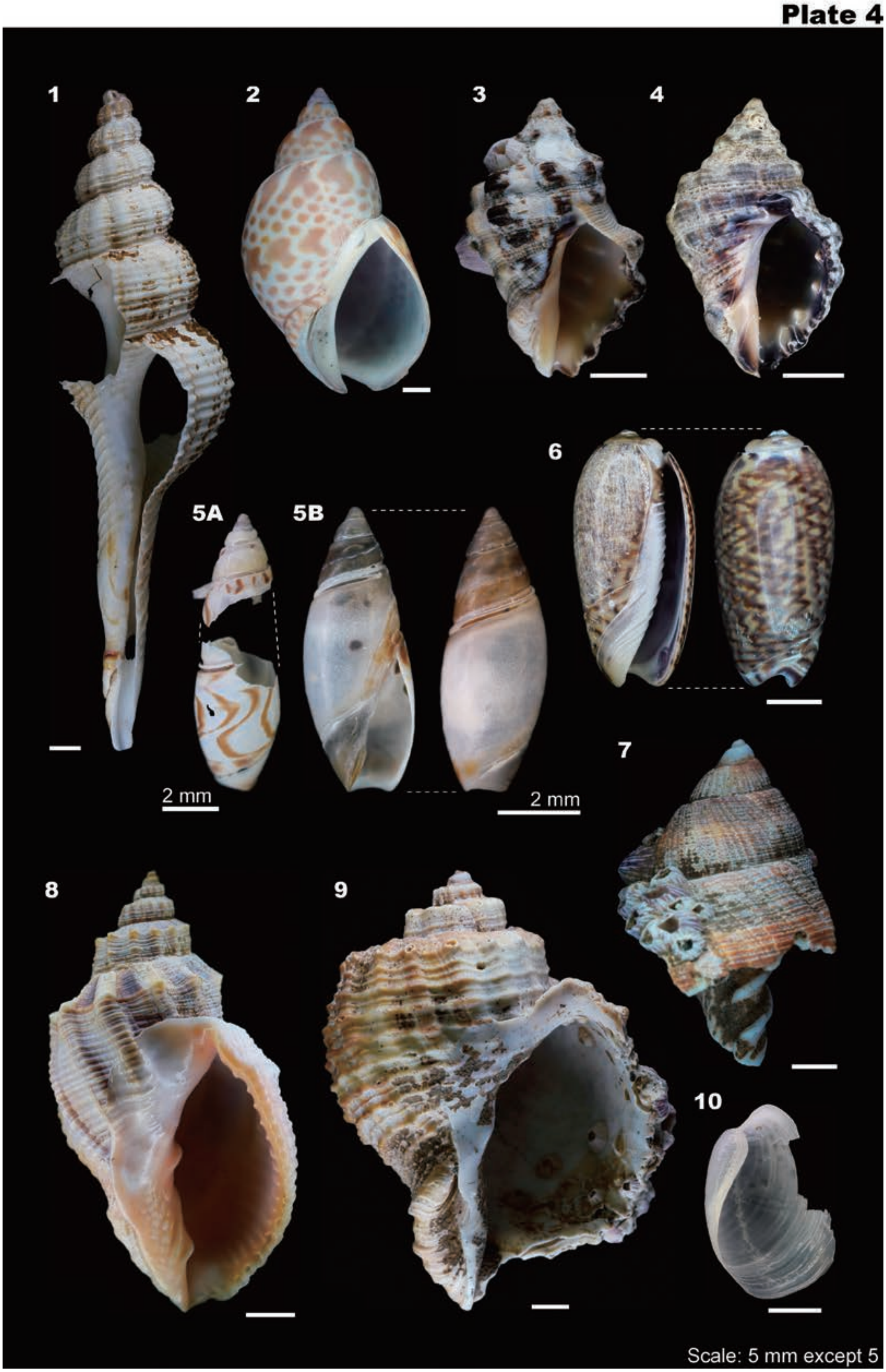
Plate 4
1
2
3
4
5A
5B
6
7
8
9
10
2 mm
2 mm
Scale: 5 mm except 5

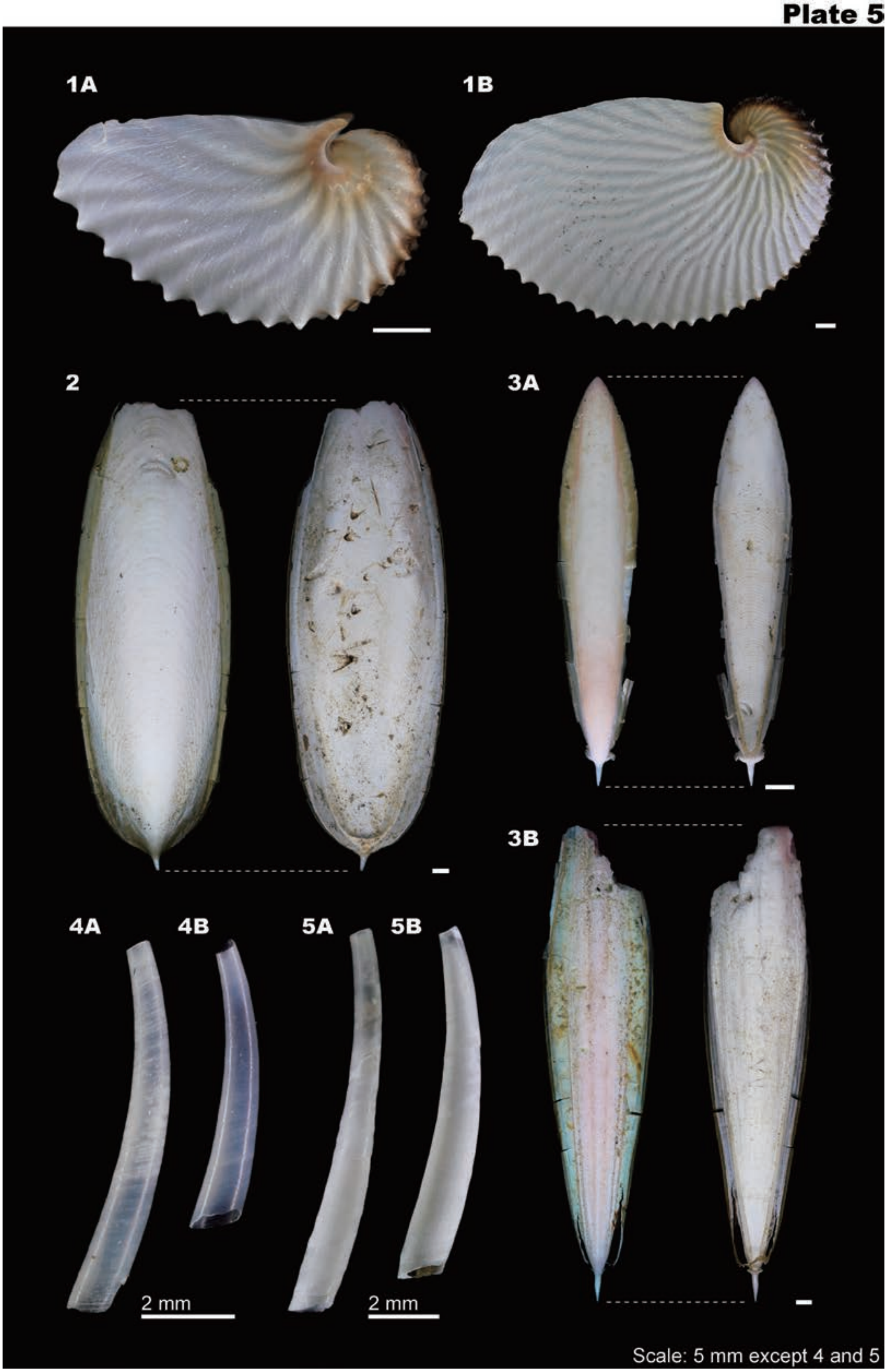
Plate 5
1A
1B
2
3A
3B
4A
4B
5A
5B
2 mm
2 mm
Scale: 5 mm except 4 and 5

Plate 6

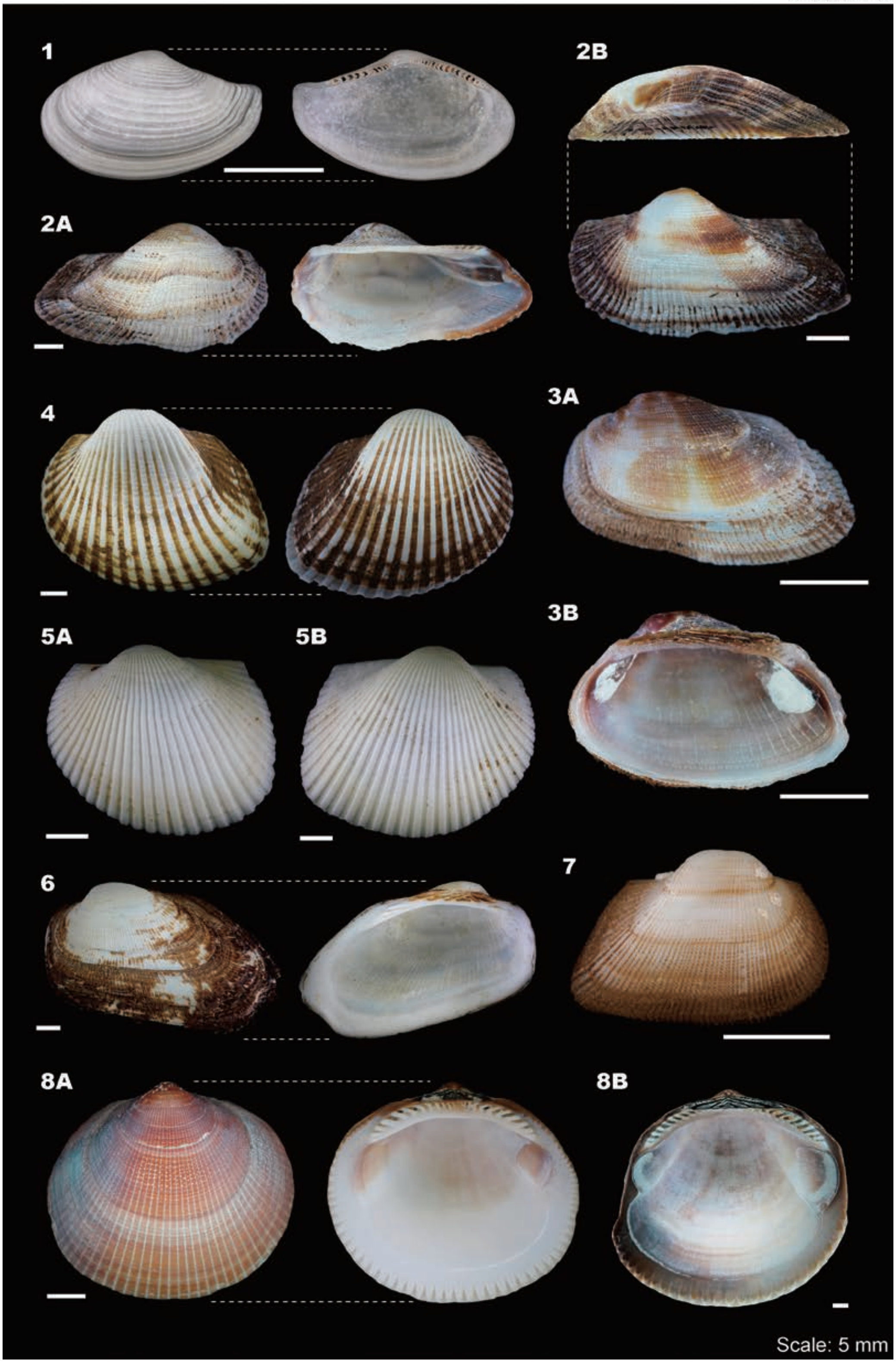

Plate 7

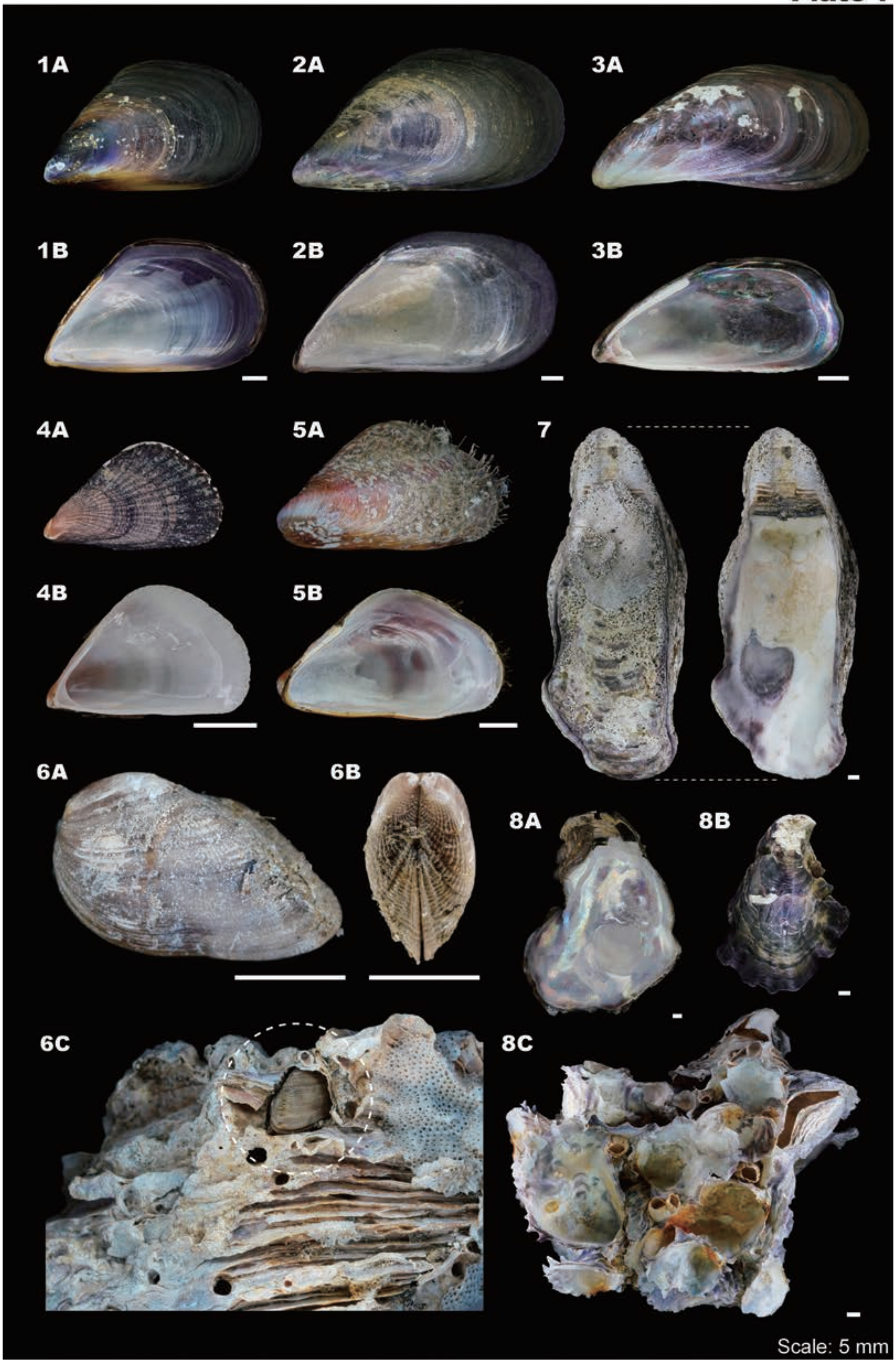

Plate 8

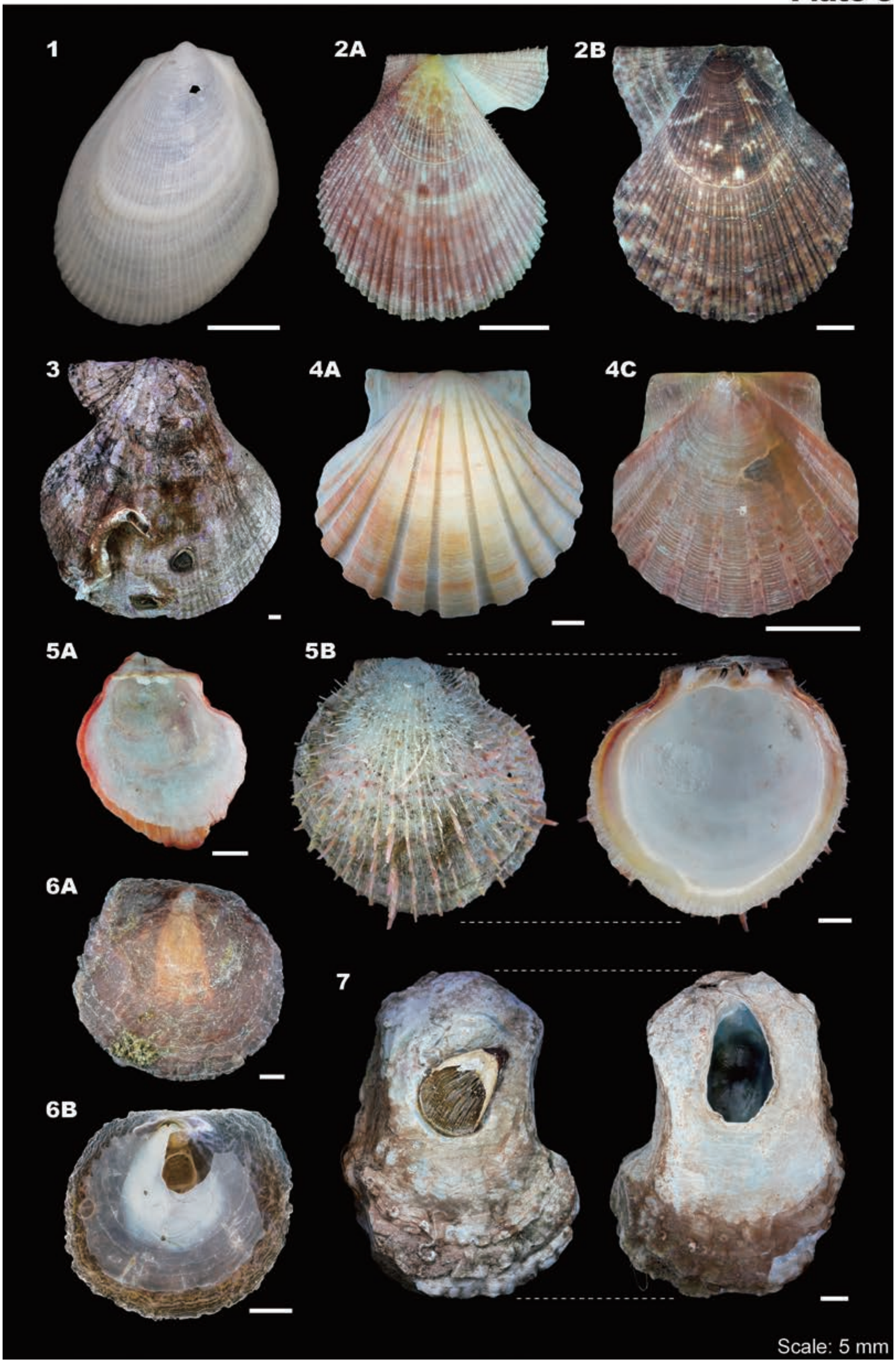

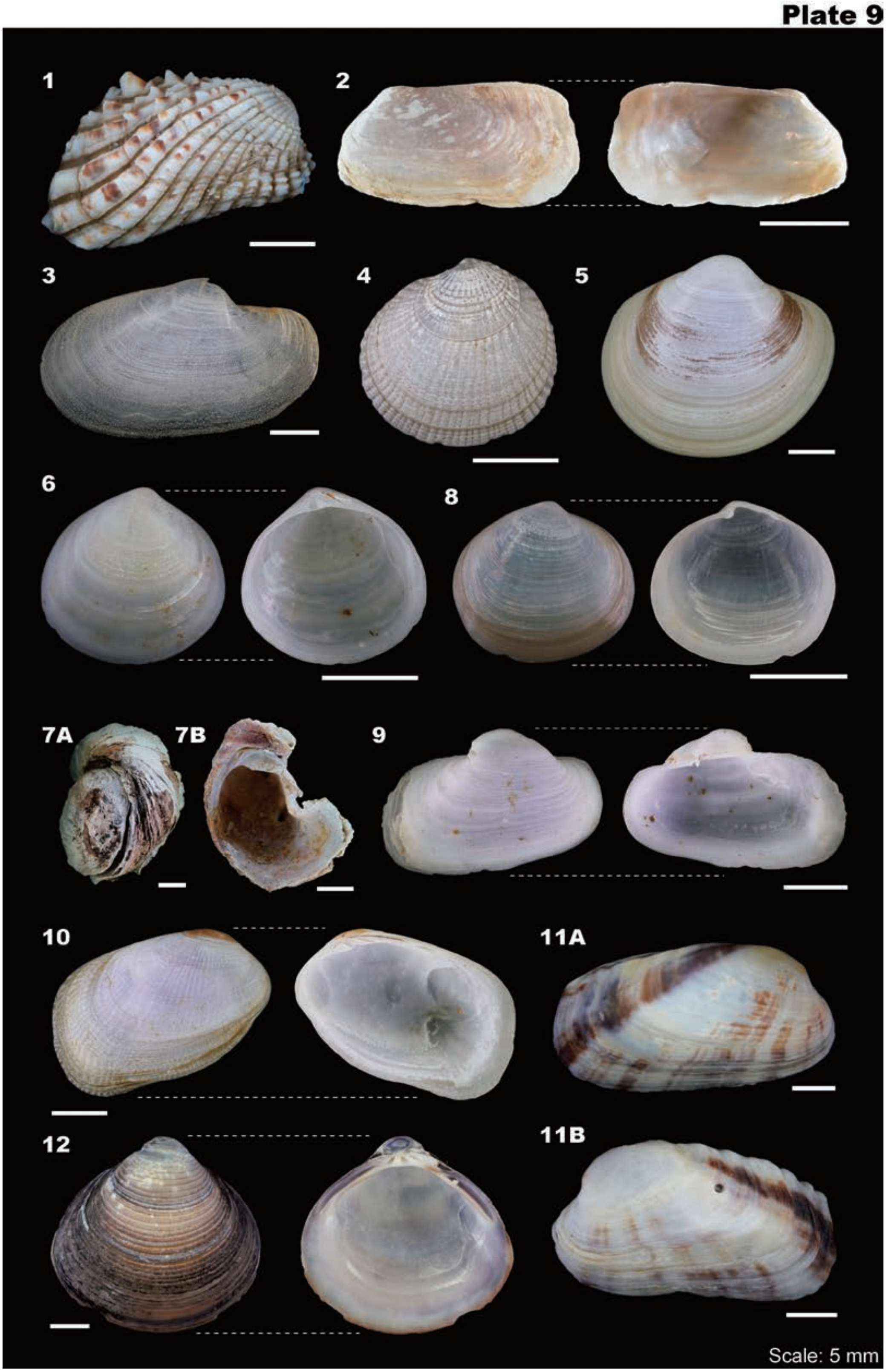
Plate 9
1
2
3
4
5
6
8
7A
7B
9
10
11A
12
11B
Scale: 5 mm

Plate 10

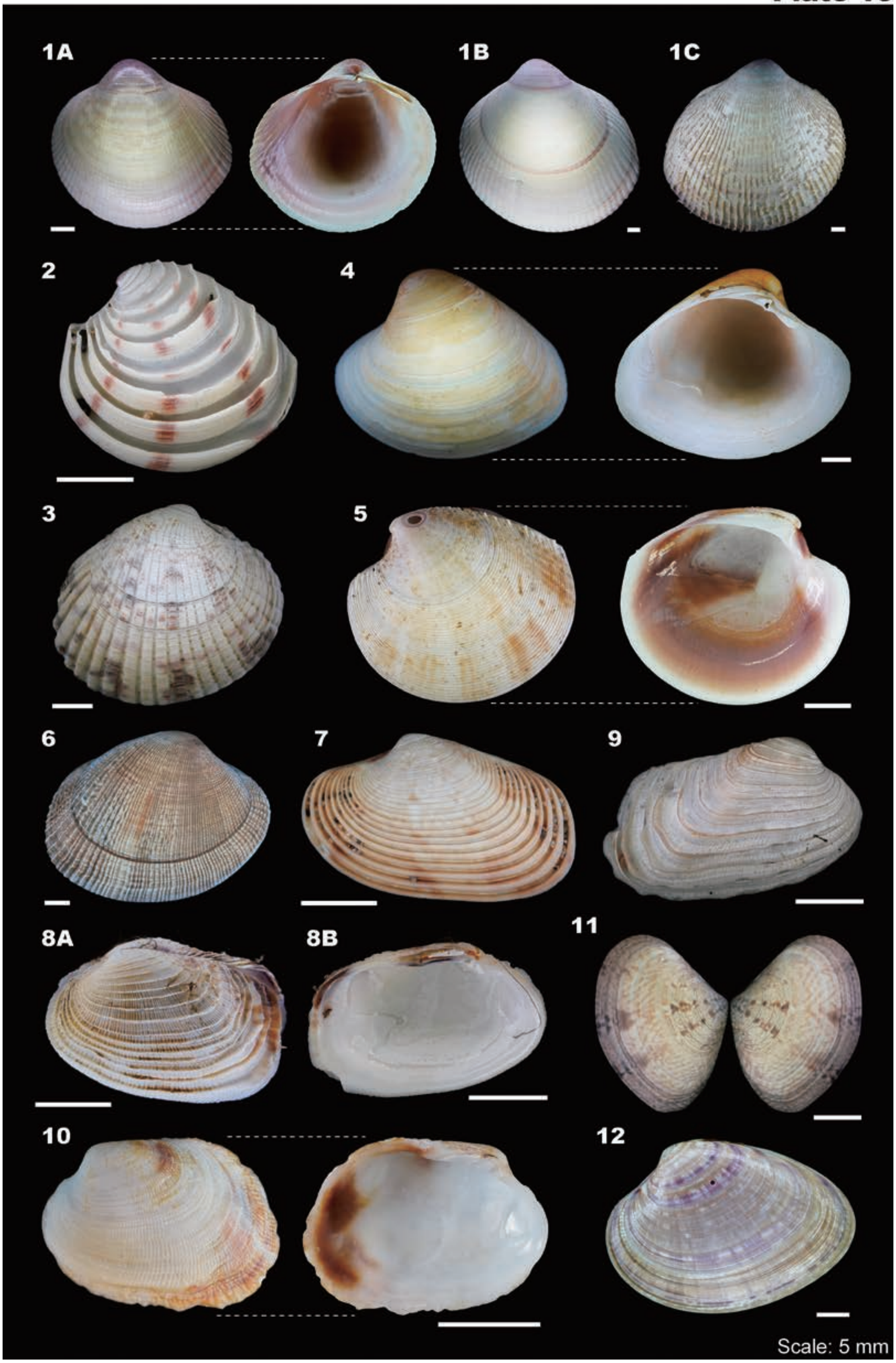

Plate 11

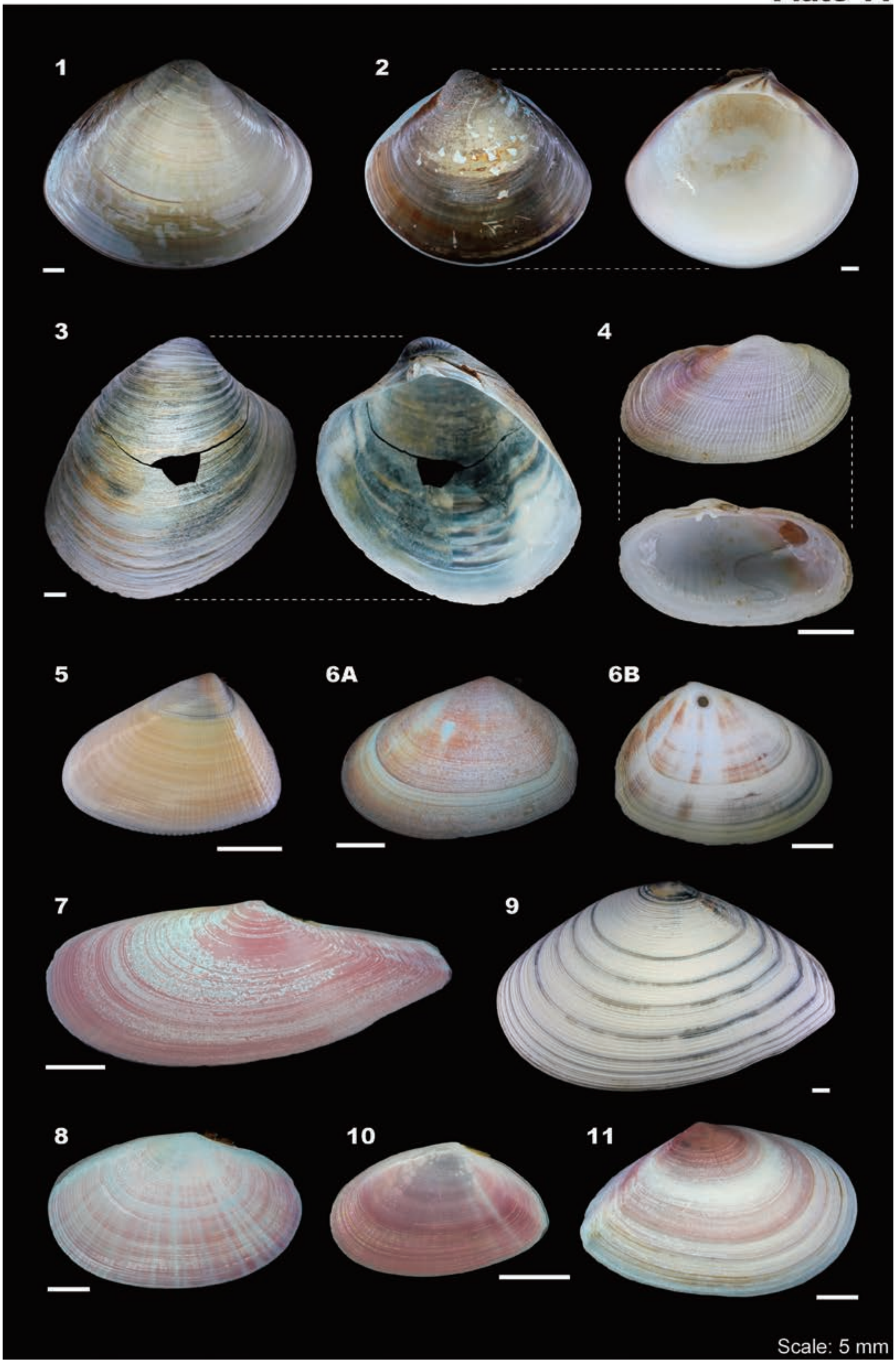

Plate 12

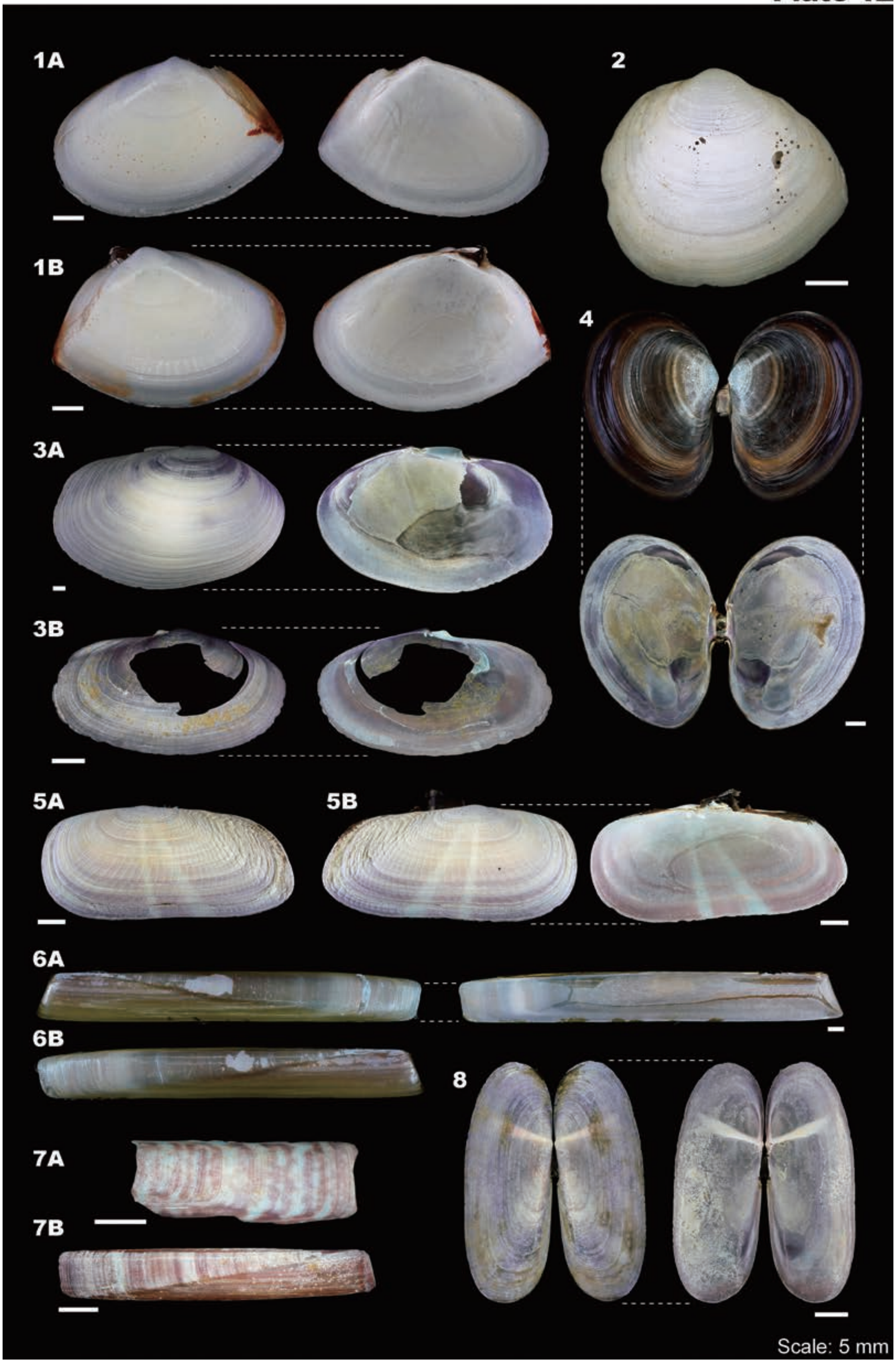

Plate 13

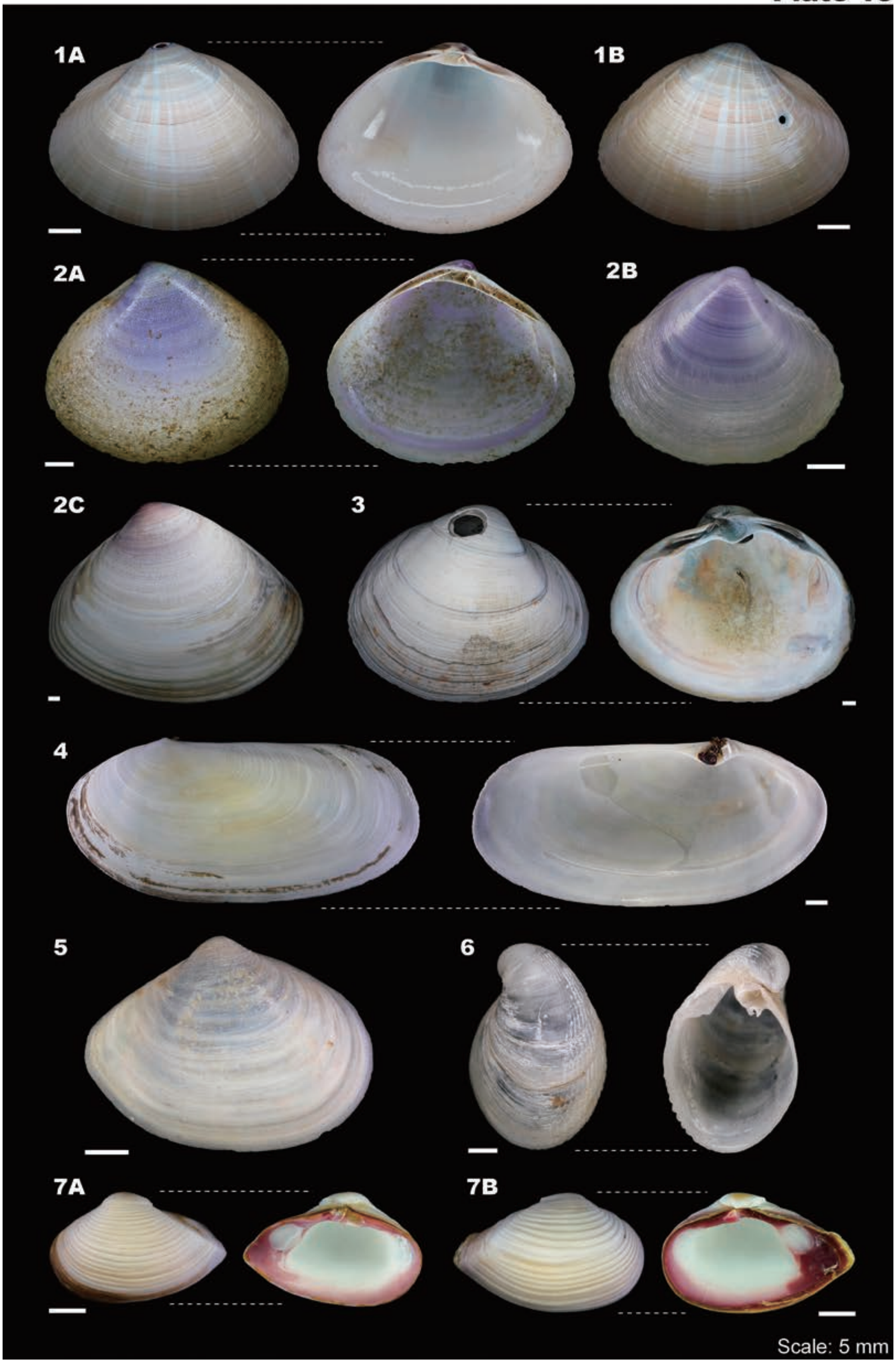

Plate 14

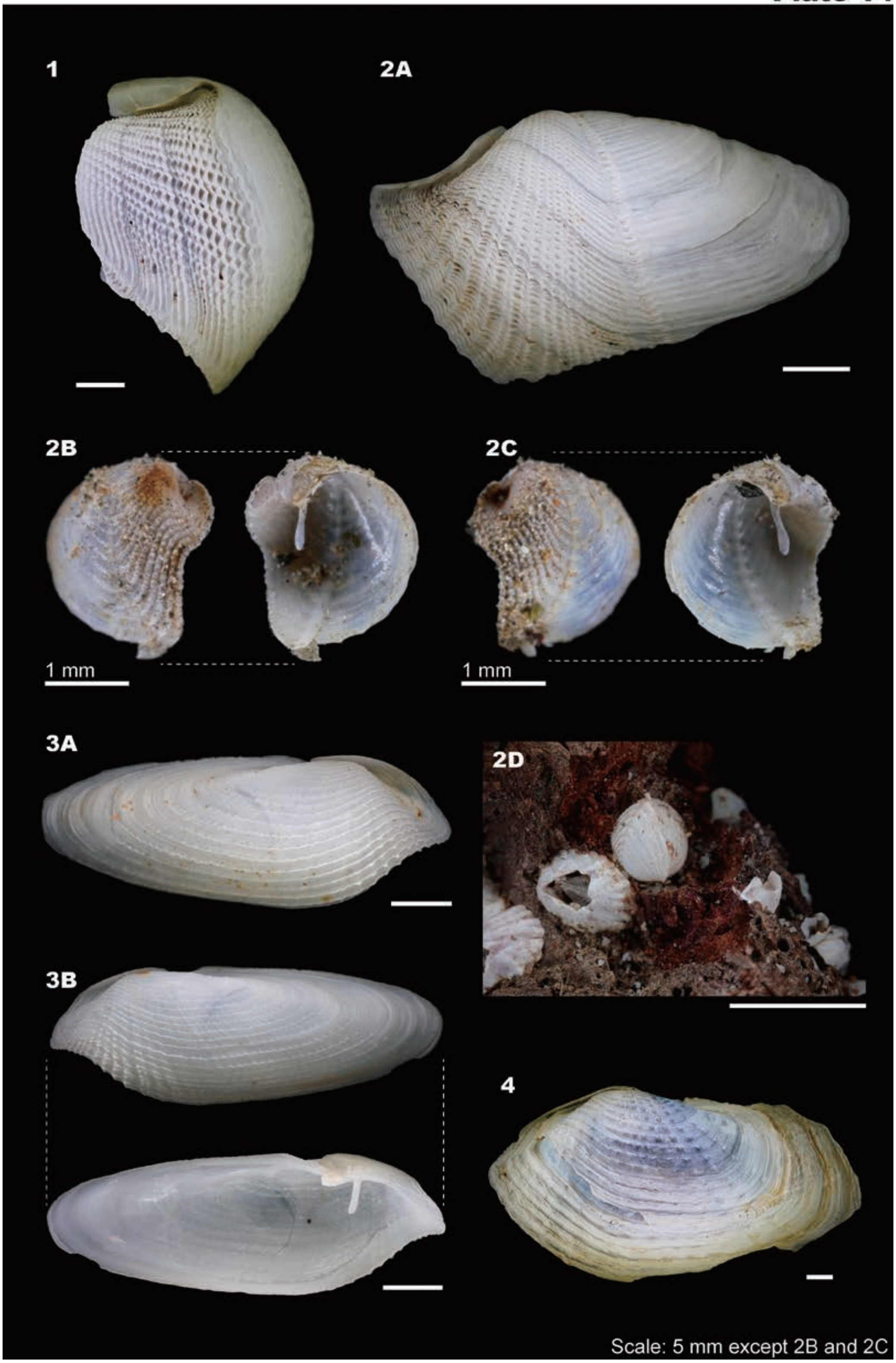

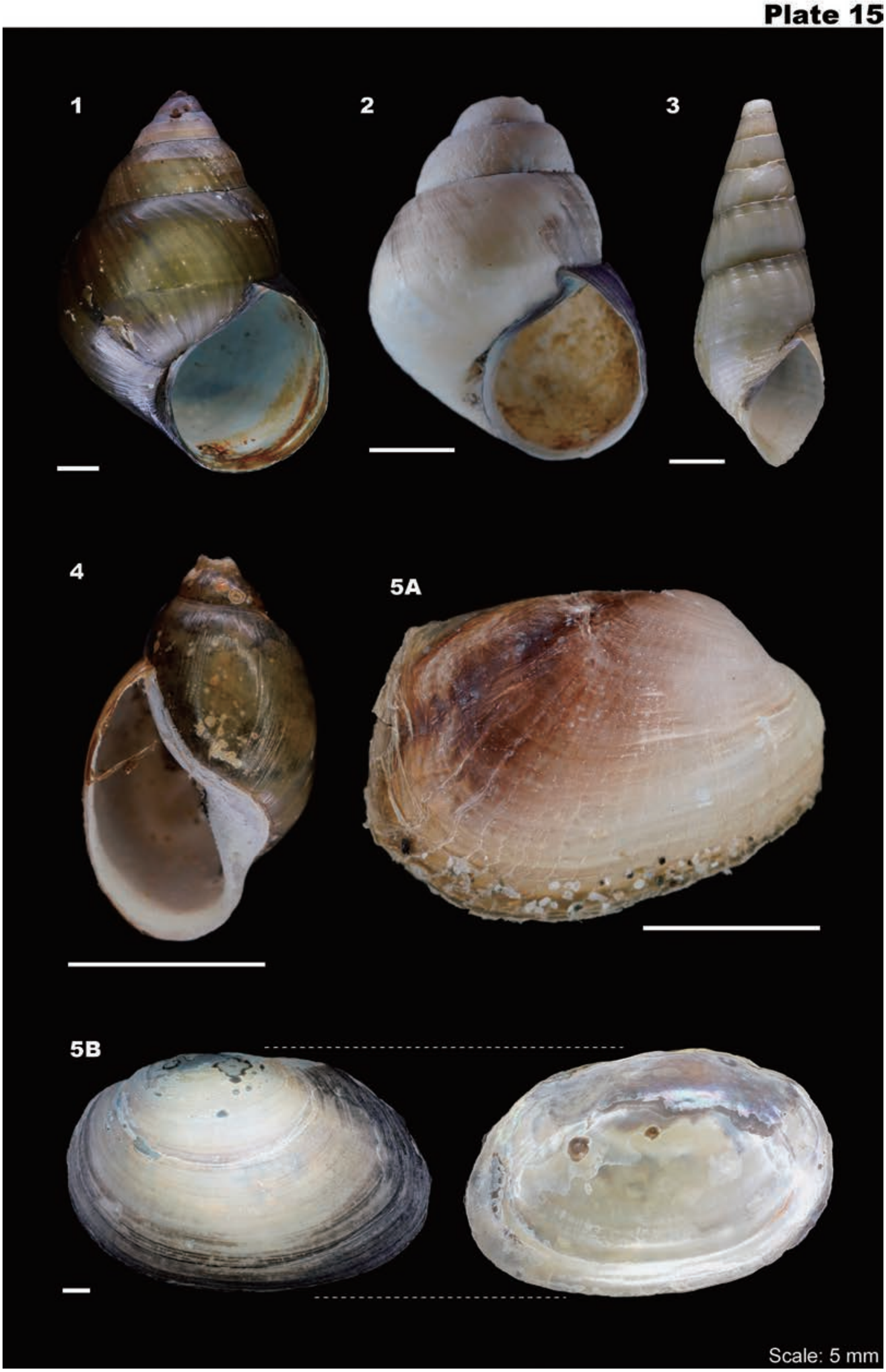
Plate 15
1
2
3
4
5A
5B
Scale: 5 mm

Promotion of responsible quarry development in line with Geopark principles in Itoigawa UNESCO Global Geopark, Niigata Prefecture, central Japan

Takuma KATORI*, Atsushi MATSUOKA**, Yu IOKAWA***,
Yousuke IBARAKI* and Theodore BROWN****

Abstract

Bodies of early Carboniferous to middle Permian limestone called Omi Limestone are widely distributed around Mt. Kurohime, Itoigawa City. Omi Limestone is not only a geological heritage of Itoigawa UNESCO Global Geopark with a high academic value, but also actively quarried for cement and carbide products, supporting industry and employment in Itoigawa for generations.

In 2020, local quarry companies announced a joint development plan for a new quarry. The basic principles of geopark activities are to conserve geological heritage and realize sustainable societies. Therefore, efforts must be made to minimize environmental impact, conserve natural resources and record those which may be lost. To that end, an academic investigation committee consisting of experts, academics and landowners was newly established within the Itoigawa Geopark Council. Under this system, several field surveys and committee meetings were held from 2020 to 2022.

To make effective use of limited natural resources and minimize the associated environmental impact, it is necessary to have opportunities for all stakeholders in the region to sit at the same table. The activity of this committee was the first opportunity for all stakeholders to exchange ideas about the balance between the conservation of natural resources and the local economy, based on the principles of UNESCO Global Geoparks. This is a significant and meaningful achievement of Itoigawa's geopark activities and represents a pioneering challenge involved in promoting responsible quarry development in line with Geopark principles for the Global Geopark Network.

Keywords: local resource conservation, responsible quarry development, Omi Limestone, Itoigawa UNESCO Global Geopark.

* Fossa Magna Museum, Itoigawa 941-0056, Japan
** Faculty of Science, Niigata University, Niigata 950-2181, Japan
*** Graduate School of Education, Joetsu University of Education, Joetsu 943-8512, Japan
**** Itoigawa Geopark Council Secretariat, Itoigawa 941-8501, Japan

Introduction

Itoigawa City records the history of the formation of the Japanese Archipelago (an island arc) and its geological diversity has nurtured rich ecosystems and culture. In recognition of its geological and cultural significance, Itoigawa Geopark became one of Japan's first three Global Geoparks (alongside Toya-Usu and Unzen Volcanic Area) in 2009. The year 2015 marked a significant milestone in the world of geological heritage conservation with the formal recognition of Global Geoparks as an official program by UNESCO. UNESCO Global Geoparks play a pivotal role in the conservation and promotion of Earth's geological heritage, fostering sustainable development, education and community engagement (UNESCO, 2015). The recognition as a UNESCO Global Geopark is contingent upon meeting specific criteria that reflect a commitment to geological heritage preservation, sustainable practices, and community involvement.

Mt. Kurohime is located in the central region of Itoigawa UNESCO Global Geopark and hosts a wide distribution of early Carboniferous to middle Permian limestone bodies called Omi Limestone (Nagamori et al., 2010). Omi Limestone is a geological heritage of high academic value, recording the growth of Paleo-Pacific reef-type limestone and environmental changes over 80 million years (Hasegawa and Goto, 1990). However, Omi Limestone is also actively quarried for cement and carbide products, supporting industry and employment in Itoigawa for generations. In 2020, as operation in the current quarry is nearing its end, local quarry companies announced a joint development plan for a new quarry. The basic principles of geopark activities are to conserve geological heritage and realize sustainable societies. Therefore, efforts must be made to minimize environmental impact, conserve natural resources and record those which may be lost. To that end, an academic investigation committee consisting of experts, academics and landowners was newly established within the Itoigawa Geopark Council to deliberate on the validity of the quarry's environmental impact assessment, as well as consider methods of investigation, recording, conservation and the impact on the lives of residents. Under this system, several field surveys and committee meetings were held from 2020 to 2022.

This paper describes the activities of the academic investigation committee on quarry development and outlines the pioneering challenges involved in promoting responsible quarry development in line with Geopark principles in Itoigawa UNESCO Global Geopark.

Geological background and topographical features of Mt. Kurohime

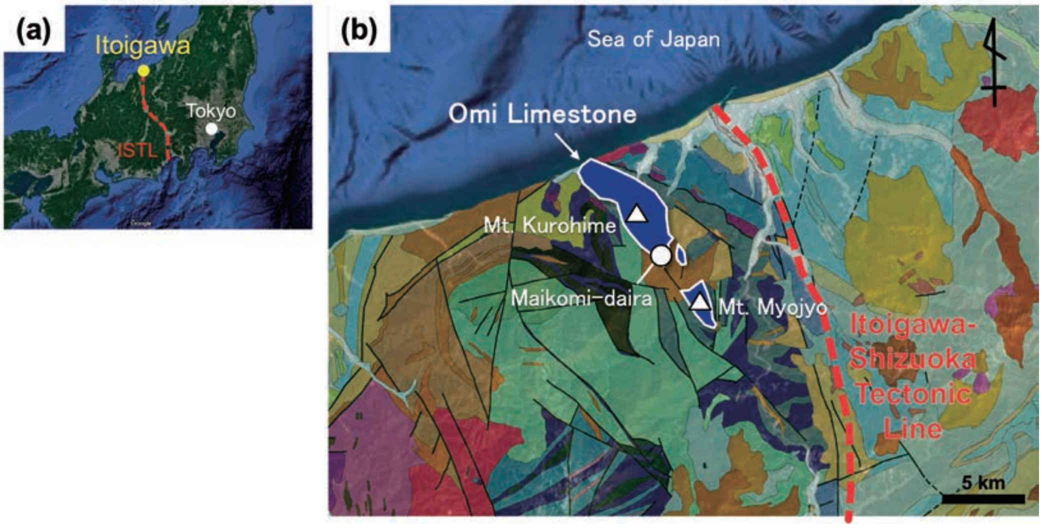

Fig. 1. (a) Index map showing the location of Itoigawa City (modified after Google map). (b) Generalized geological map around the centre of Itoigawa City (modified after Seamless Digital Geological Map of Japan published by Geological Survey of Japan, AIST). Highlighted blue shows the distribution of Omi Limestone. Location of the Itoigawa-Shizuoka Tectonic Line (ISTL) is shown by red line.

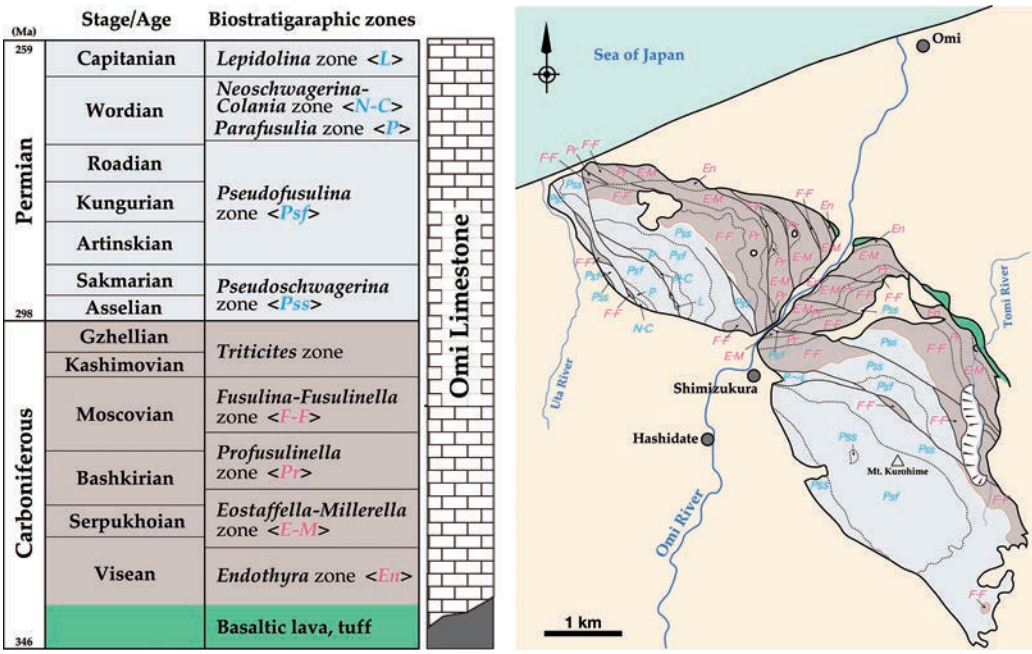

Fig. 2. Stratigraphic distribution and distribution map of fusulinids in Omi Limestone (Nagamori et al., 2010) after Hasegawa and Goto (1990). Stages and ages referred to Cohen et al. (2013).

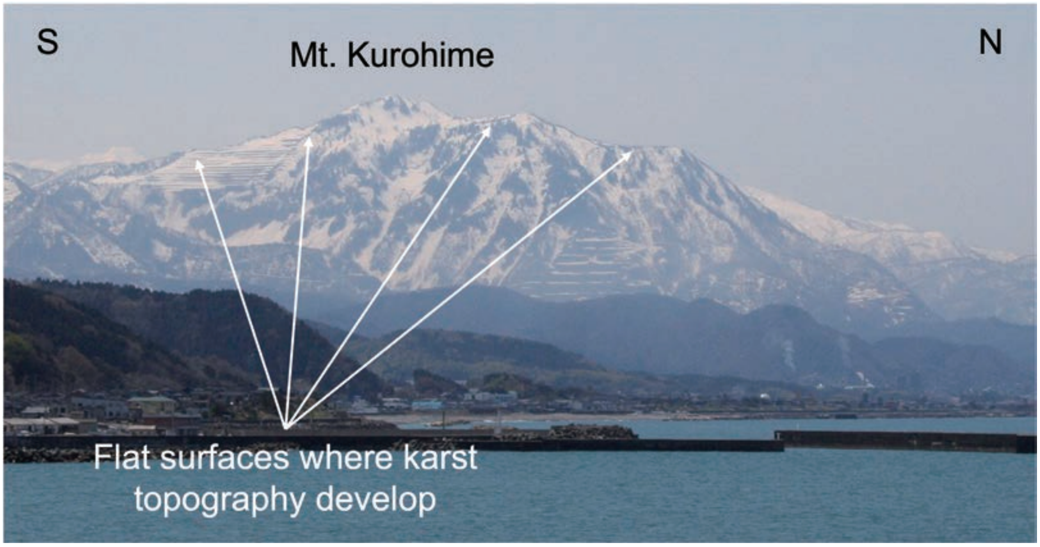

Fig. 3. View of Mt. Kurohime from the Uramoto Coast.

Mt. Kurohime (1,221 m) is composed of a Carboniferous-Permian limestone body called Omi Limestone (Figs. 1 and 2). It is one of giant limestone bodies in the Akiyoshi terrane, a geologic entity in the Inner zone of Southwest Japan. These giant limestone bodies are Akiyoshi, Taishaku, Atetsu and Omi, representing a distance of over 1,000 km from Yamaguchi Prefecture in the west to Niigata Prefecture in the east. They are regarded as seamount cap originated in the Panthalassic Ocean in the late Paleozoic. The bodies record a long-term history in the pelagic environments in the Panthalassic Ocean from early Carboniferous to middle Permian over the span of up to 80 million years. Fossil records of various biota in the limestone bodies have a potential to reveal their evolutionary history in pelagic reef environments. Detailed biostratigraphic research on benthic foraminifer has been performed on Omi Limestone (Hasegawa and Goto, 1990).

Another aspect of Omi Limestone is its topography. Karst topography is formed in limestone by water erosion and sometimes forms deep vertical caves (Fig. 3). The most representative vertical caves around Mt. Kurohime are found in Maikomi-daira, which is located on the south side of the summit (Fig. 1b). Figure 4 shows a schematic cross-sectional view of Maikomi-daira and lists the depth ranking of vertical caves in Japan. Maikomi-daira has many vertical caves, including the 4 deepest vertical caves in Japan (Fig. 4), making it one of the country's representative karst topographies. Due to this particular topography, it is also home to many precious animals and plants. For these reasons, it is protected as a Prefectural Environmental Conservation Area. In order to conserve and utilize this valuable heritage, Itoigawa Geopark Council operates environmentally responsible tours in partnership with local organizations. To avoid overtourism and reduce environmental impact, these tours are limited to no more than 10 per year, held at intervals of at least two weeks. From 2019 until 2022 the access road to this site was closed due to typhoon damage,

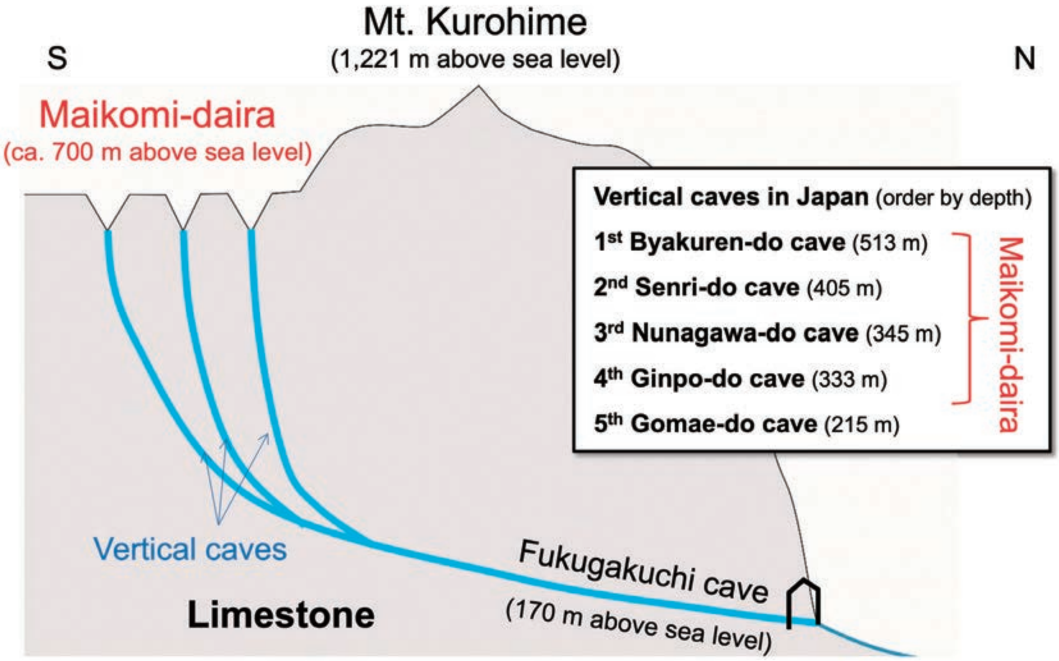

Fig. 4. Schematic cross-sectional view of Maikomi-daira and list of vertical caves in Japan by depth.

but tours have restarted since the 2023 season, and are as popular as ever.

It is important to note that as a Conservation Area, Maikomi-daira is excluded from the quarry development area, but care will have to be taken to assure that nearby quarry development does not negatively affect protected sites.

Academic investigation committee in response to quarry expansion

In Itoigawa City, there are two large companies engaged in quarrying around Mt. Kurohime. One is Denka CO., Ltd., established in 1921, and the other is Myojyo Cement CO., Ltd., established in 1958. The south side area with steps on the mountain is the current quarry of Myojyo Cement (Fig. 3). The limestone quarried around Mt. Kurohime is used not only as a raw material for cement, but also as a raw material for carbide products, and has supported industry and employment in Itoigawa for generations. In 2020, as operation in the current quarry is nearing its end, these two companies have announced a joint development plan for a new quarry.

In Japan, there are strict laws that must be cleared when developing quarries, and development can only start if criteria such as the completion of an environmental impact assessment are cleared. However, both Denka and Myojyo Cement are aware of the local Geopark's efforts to protect and conserve natural heritage, therefore, they have provided the City of Itoigawa an opportunity to evaluate the area's academic value and to pass on that value to future generations.

Table 1. List of the Academic Investigation Committee membership. Affiliation and position are as of the time of the committee.

	Name	Position, Affiliation	Subcommittees
Member	Atsushi MATSUOKA	Professor, Niigata University	topography/geology
	Toshiyuki KURIHARA	Associate professor, Niigata University	
	Kotaro YAMAGATA	Professor, Joetsu University of Education	
	Katsunori FUKUI	Professor, University of Tokyo	
	Yu IOKAWA	Professor, Joetsu University of Education	flora/fauna
	Hiroshi YASHIKI	Member, The Mammal Society of Japan	
	Jun HASHIZUME	Senior researcher, Niigata Prefectural Museum of History	archaeology/history
	Tsutomu KIJIMA	Director, Chojagahara Archaeological Museum	
	8 other members	Landowners etc.	-
Observer	Denka CO., Ltd.		
	Myojyo Cement CO., Ltd.		
	Taiheiyo Cement CO., Ltd.		
	Joetsu Environmental Science Center		
	Agency for Cultural Affairs, Government of Japan		
	Ministry for the Environment		
	Cultural Affairs Division, Niigata Prefectural Government		
	Land Use Division, Niigata Prefectural Government		
	Environmental Policy Division, Niigata Prefectural Government		
	Itoigawa Regional Development Bureau, Niigata Prefectural Government		
Secretariat	Itoigawa Geopark Council Secretariat		

An academic investigation committee was newly established within the Itoigawa Geopark Council to deliberate on the validity of the results of the environmental impact assessment, including its methods of investigation, recording, conservation and the expected impact on the lives of local residents. The members of the committee are shown in Table 1. The committee consists of experts such as university professors and landowners. In addition, related national ministries, agencies and prefectural departments participated as observers. Under this system, from 2020 to 2022, several field surveys and committee meetings were held.

In this committee, three subcommittees focusing on topography/geology, flora/fauna and archaeology/history were established to delve into discussions within their respective domains. While this paper does not provide detailed results from each subcommittee, considering perspectives such as nature conservation, the environmental impact and value of the quarry site could be discussed academically and specifications and systems for mitigating environmental impact and recording lost resources could be established. The summary regarding conservation efforts for quarry development within the committee was passed to Itoigawa City in 2022 as follows:

1. Scientific evaluation and validity of natural and cultural resources in Omi Limestone

The committee assessed the validity of the environmental impact assessment (self-assessment) conducted by the quarry companies. As a result, the surveyed contents were deemed to meet the requirements as laid out by prefectural ordinance and the contents of the environmental conservation measures were considered generally valid. In order to evaluate the scientific value of natural and cultural resources in Omi Limestone, the committee conducted additional investigations to address deficiencies identified in the self-assessment. The results of the self-assessment and the committee's investigations suggest the potential presence of significant features in Omi Limestone, including Japan's deepest vertical caves, well-developed karst topography unique to snowy regions and traces of prehistoric human utilization. Additionally, the distinctive terrain supports the existence of valuable subalpine flora and mammals, contributing to its remarkable scientific value in Japan.

2. Evaluation and validity of conservation and development areas in Omi Limestone

As mentioned above, the vicinity of Mt. Kurohime holds remarkable scientific value in Japan, associated with legends rooted in its topography and serving as a stage for mountain worship. Particularly, Maikomi-daira's designation as a Niigata Prefectural Natural Environmental Conservation Area, acknowledges numerous natural and cultural resources representative of Omi Limestone, establishing its exceptionally high scientific value. For this reason, it is deemed appropriate to strength Maikomi-daira's designation as a legally protected area, with the assumption of necessary environmental conservation measures based on the records of the development area, justifying the development plan in the designated area. It is also suggested to consider designating Maikomi-daira as a National Natural Monument, proposing further sustainable conservation methods.

3. Examination and implementation of academic surveys for record and conservation

Detailed investigation of natural resources lost due to development is academically significant. Therefore, from a scholarly perspective, surveys of the shapes, sediments, and plant life within representative dolines and geological stratigraphy are proposed. The accumulated data, rocks, and boring cores should be centralized and stored in facilities such as the Itoigawa City's Fossa Magna Museum, enabling academic utilization. Moreover, insights gathered about future natural and cultural resources can be considered for display in museums and exploration as geopark resources.

4. Impact on the Lives of Local Residents

The items covered in the environmental impact assessment are deemed to meet the requirements laid out by prefectural ordinance, with minimal impact on residents' lives. It should be noted as commendable that after conducting hearings and explaining the content and results of the self-assessment to residents, further investigations were conducted on items identified as lacking (such as water quality). However, thorough measures to ensure the safety of residents during the transportation of large materials, considerations for noise and continuous monitoring of water quality and quantity at predicted impact points are necessary.

5. Framework for Future Conservation Systems

To continue the conservation of natural and cultural resources, it is essential to establish a framework that aligns with the progress of development and the content of record conservation. Preparations for the period leading up to mining include activities such as deforestation, topsoil removal, and bench formation, which are expected to change the current terrain rapidly compared to post-quarrying activities. Therefore, several surveys, primarily focusing on terrain and biodiversity, are anticipated. For this reason, there is a need to promptly establish a new ongoing survey committee and develop a framework that can respond to continuous investigations. Following the commencement of quarry activities, when geological stratigraphy will be the primary focus, and considering the extended project duration, it is deemed appropriate for the local government and the quarry companies to collaborate on continuous surveys, incorporating expert opinions. Furthermore, when planning the next development, it is hoped that a framework similar to this committee, allowing discussions on the environmental impact and conservation and utilization of regional resources, will be established.

Responsible quarry development in line with Geopark principles

Although quarry development leads to the loss of natural resources, it is an important industry that has supported the local economy and employment for over one hundred years. One means of balancing conservation and development is to draw a line between areas to be conserved and areas to be developed based on their academic value. While this method is clear, it potentially creates division between the two sides. To make effective use of limited natural resources and minimize the associated environmental impact, it is necessary to have opportunities for all stakeholders in the region to sit at the same table. Until now, there had never been an opportunity to dialogue with quarry companies at such a level. This committee created a valuable first opportunity for all stakeholders to exchange ideas about the delicate balance between natural resource conservation and local economic development, based on the principles of UNESCO Global Geoparks. It is the authors' belief that this is a significant and meaningful achievement of geopark activities within the City of Itoigawa and represents a new opportunity to proactively promote a sustainable society which strikes an effective balance between conservation and responsible development to meet the needs of local stakeholders and residents.

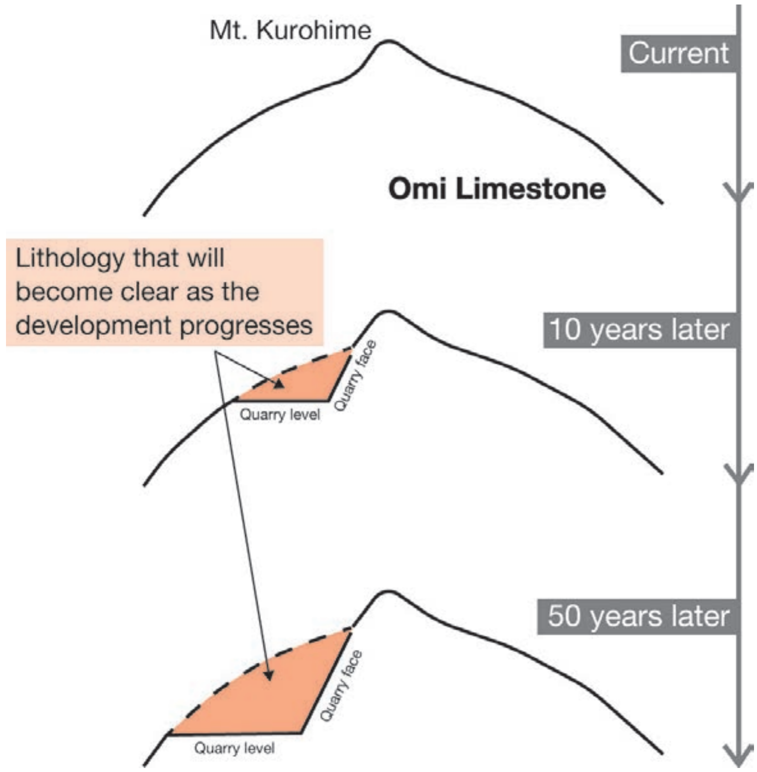

Fig. 5. Conceptual image of layered records of lithology that will become clear as the development progress.

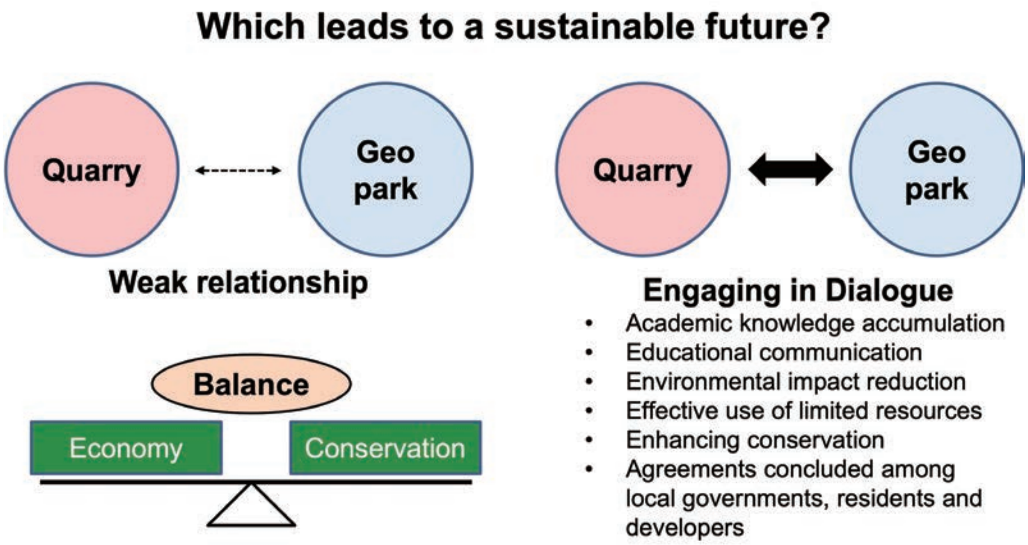

Fig. 6. Diagram illustrating the relationship between quarry companies and Itoigawa Geopark. On the left is the relationship before the establishment of this committee in 2020. On the right is the relationship after the establishment of this committee in 2020.

Concluding remarks

The authors strongly concluded that it is necessary to continue academic investigations and environmental conservation monitoring of the quarry activities in accordance with the progress of development. A successor committee was established in 2022 to continue this investigation and conservation work. For example, efforts are being made to relocate populations of low-migratory mice and rare plants to preserve regional biodiversity. In addition, a plan is in place to obtain layered records of lithology that will become clear as the development progresses (Fig. 5). With the cooperation of a research institute, quarry company and the Itoigawa Geopark Council, field surveys, rock sampling and UAV monitoring of the quarry-face will be conducted in accordance with development progress. These monitoring surveys are expected to contribute significantly not only to academia but also to the promotion of science education (Fig. 6).

Acknowledgements

We thank the committee members and observers for their constructive discussion. We also thank Denka CO., Ltd., Myojyo Cement CO., Ltd., and Taiheiyo Cement CO., Ltd., for their help in the committee management and the manuscript review. Constructive reviews by Toshiyuki Kurihara are highly appreciated.

References

Cohen, K.M., Finney, S.C., Gibbard, P.L. and Fan, J.-X., 2013 (updated), The ICS International Chronostratigraphic Chart. *Episodes,* **36**, 199–204.

Hasegawa, Y. and Goto, M., 1990, Paleozoic and Mesozoic of Omi region. Guidebook of Field Excursion at 97th Meeting of the Geological Society of Japan, 227–260 (in Japanese).

Nagamori, H., Takeuchi, M., Furukawa, R., Nakazawa, T. and Nakano, S., 2010, Geology of the Kotaki District. Quadrangle Series, 1:50,000, Geological Survey of Japan, AIST, 130 p. (in Japanese with English abstract).

UNESCO, 2015, *Statutes of the International Geoscience and Geoparks Programme and Operational Guidelines for UNESCO Global Geoparks*. UNESCO, Paris, 6 p.

CONTENTS

Ⓒ **DEPARTMENT OF GEOLOGY, FACULTY OF SCIENCE, NIIGATA UNIVERSITY**
8050 Ikarashi Nino-cho, Nishi-ku, Niigata 950-2181, Japan
TEL +81-(0)25-262-6197 FAX +81-(0)25-262-6194